Geofísica Internacional (1996), Vol. 35, Num. 4, pp. 377-401

Seismic structure between the Pacific coast and Mexico City from the Petatlán earthquake (M_S=7.6) aftershocks

Carlos Valdés-González[1] and Robert P.Meyer[2]
[1] *Instituto de Geofísica, UNAM., México, D.F., México.*
[2] *Department of Geology and Geophysics, University of Wisconsin, Madison, USA.*

Received: November 16, 1995; accepted: August 1, 1996.

RESUMEN

Los tiempos de arribo de ondas P y S de las réplicas del sismo del 14 de marzo de 1979 Petatlán (M_s=7.6), han sido usados para delinear una estructura de velocidades compresionales y de corte para la zona de subducción entre Petatlán y la ciudad de México y a lo largo de la costa del estado de Guerrero. El modelo final consiste en una zona de transición bidimensional, compuesta por un bloque continental, uno acrecional y uno de corteza oceánica. El bloque continental consiste en tres capas corticales planas con el Moho localizado a 45 km de profundidad. El bloque oceánico fue modelado con dos capas con un espesor total de 8 km y con un echado de 10° al N34°E, que se extiende tierra adentro. Las ondas sísmicas de las réplicas con hipocentros debajo de la corteza oceánica viajan principalmente en el manto oceánico superior y alcanzan sitios entre los 50 y 300 km tierra adentro.

La localización hipocentral de 792 réplicas fue comparada con la estructura obtenida con el trazado de rayos. Tres por ciento de estas réplicas se localizan dentro de la región sugerida como el bloque continental, 85% están dentro de la corteza oceánica y 12.5% debajo de la corteza oceánica. 55% de los eventos se localizan bajo el arreglo sísmico local y sus hipocentros están determinados con errores menores de 5 km.

Los hipocentros de las réplicas definen una zona angosta de Wadati-Benioff con 8-10 km de espesor, la cual concuerda con el modelo de la litosfera oceánica basada en los tiempos de viaje de las réplicas registradas por el perfil sísmico a lo largo de la costa y en dirección a la ciudad de México. 50% de las réplicas (aproximadamente 350) se encuentran dentro de la corteza oceánica en una capa delgada de menos de 8 km de espesor y con un área de 480 km^2 localizada a mayor profundidad y alejada de la trinchera. Esta es una región localizada principalmente bajo las estaciones sísmicas y ha sido propuesta como una zona de fuerte acoplamiento en una litosfera joven y de rápida convergencia (Astiz, 1987; McNally *et al.*, 1986), y como una asperidad basada en la localización de los premonitores del sismo de Petatlán (Hsu *et al.*, 1984) y también en sus réplicas (Valdés *et al.*, 1982; Hsu *et al.*, 1984).

PALABRAS CLAVE: Réplicas, zona de subducción, modelo de corteza, trazado de rayos y asperidad.

ABSTRACT

P- and S-wave travel times from aftershocks of the M_s=7.6 Petatlán, Guerrero, Mexico earthquake of March 14, 1979, have been used to delineate a compressional- and shear-wave velocity structure of the subduction zone between Petatlán and Mexico City and along the coast of the State of Guerrero. The final model consists of a two-dimensional ocean-to-continent transition zone composed of a continental, an accretionary and an oceanic crust block. The continental block as modeled consists of three flat crustal layers with the Moho at 45 km depth. The oceanic crust is modeled as two layers with 8 km total thickness, dipping 10° at N34°E, and extends well inland. Seismic waves from aftershocks with hypocenters below the oceanic crust travel principally in the oceanic upper mantle to sites between 50 and 300 km inland.

The hypocentral location of 792 Petatlán aftershocks was compared with the structure obtained by ray tracing. Three percent of those aftershocks are located within the suggested continental block, 85% are within the oceanic crust and 12.5% are below the oceanic crust. 55% of them are located under the local array and their hypocenters are constrained to within ±5 km.

The hypocenters of the aftershocks define a narrow, 8-10 km wide Wadati-Benioff zone that agrees with the model of oceanic lithosphere based on travel times from aftershocks recorded by profiling arrays along the coast and toward Mexico City. 50% of the aftershocks within the oceanic crust (approximately 350) are concentrated in a thin sheet less than 8 km thick with an area of 480 km^2 and located deeper and away from the trench. This is a region largely under the recording array and has been proposed to be a region of strong coupling in young and fast convergence rate subducting lithospheres (Astiz, 1987; McNally *et al.*, 1986) and an asperity based on the location of the Petatlán earthquake foreshocks (Hsu *et al.*, 1984) and also aftershocks (Valdés *et al.*, 1982; Hsu *et al.*, 1984).

KEY WORDS: Aftershocks, subduction zone, crustal model, ray tracing and asperities.

INTRODUCTION

Southwestern Mexico is the site of large thrust earthquakes related to the subduction of the Cocos plate beneath the North America plate (Figure 1). The Middle America Trench (MAT), north of the Tehuantepec ridge, parallels the coast at distances of 70 to 100 km. There have been 42 earthquakes here since the turn of the century, but knowledge and understanding of the ocean-to-continent transition structure has remained poor. In early March, 1979, just before the Petatlán earthquake, as part of the Rivera Oceanographic Seismic Experiment (ROSE), the University of Wisconsin-Madison group was in the State of Guerrero preparing to deploy its newly designed digital recording seismographs. On March 14, a earthquake occurred offshore near Petatlán. Two days after the main shock, a team from

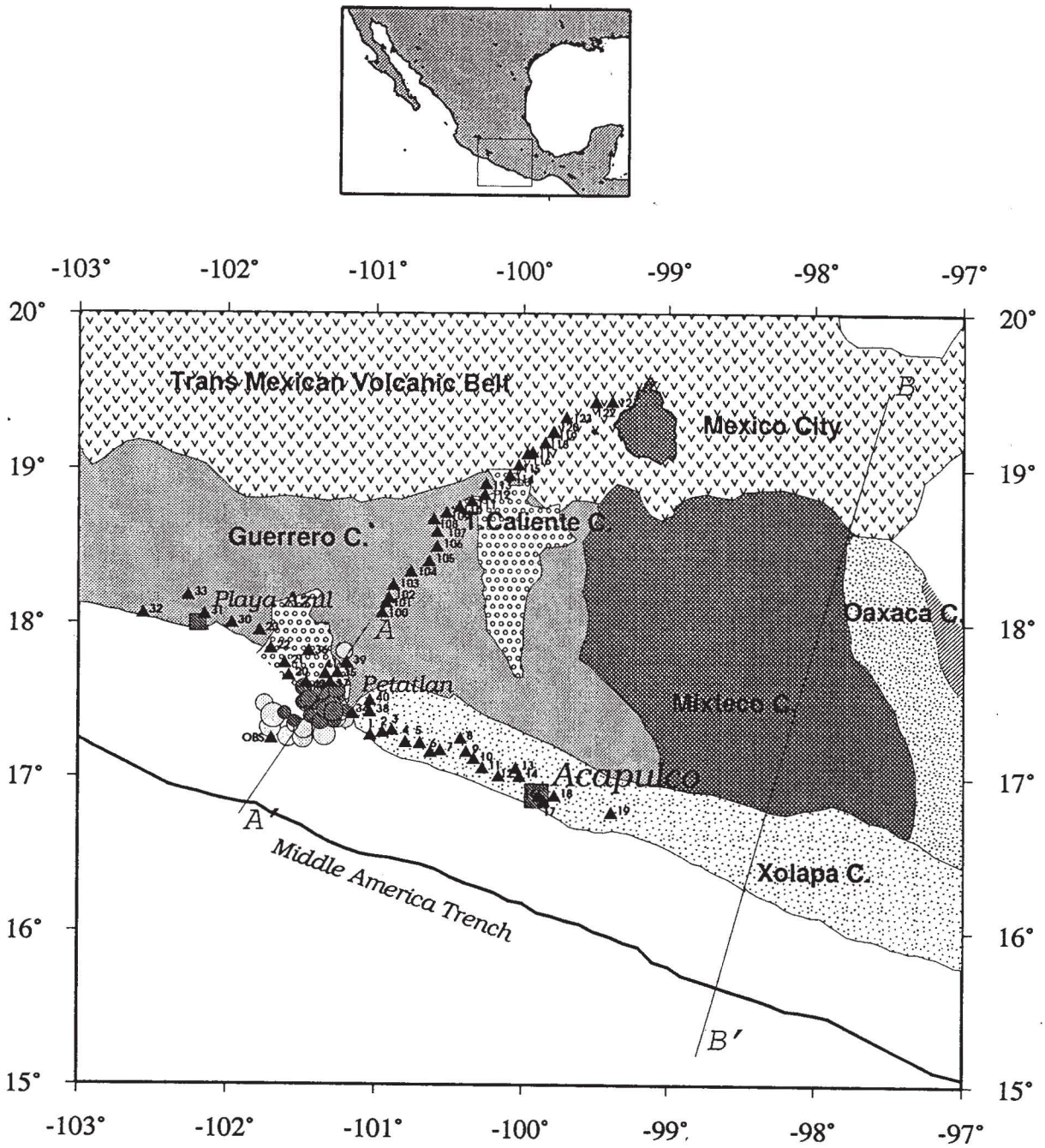

Fig. 1. Epicentral map of 36 aftershocks located using only seismographs in the Petatlán area (solid triangles, stations 35-41) and also recorded by up to 4 seismographs along the coast toward Acapulco (stations 1-19) and toward Playa Azul (stations 20-33), and toward Mexico City (stations 100-123). Numbers identify seismographs in Figures 3-15. Open circles correspond to aftershocks recorded by the Petatlán-Mexico City profile, and solid circles to aftershocks recorded by the Petatlán-Acapulco and Petatlán-Playa Azul coastal profiles. These aftershocks have Mc from 1.6 to 4.1, with an origin time mean RMS of 0.27 s, and horizontal and vertical standard errors of 2.91 and 5.72 km, respectively. The line A-A' indicates the cross section shown in Figure 4. Line B-B' indicates the Oaxaca profile referred on the text. The selection criteria for these aftershocks, was that they were aligned with and recorded by as many seismographs along the profiles as possible. The geology, from Ortega-Gutiérrez (1981) and López-Ramos (1976, 1983) of the area is indicated by zones with different patterns.

the Universities of Mexico and Wisconsin had installed 16 seismographs in the aftershock area (Valdés *et al.*, 1982). In addition, 8 digital recording instruments were deployed in a leap-frog fashion along two profiles, one between Petatlán at the Pacific Coast and Mexico City (Pet-Mex) and the other, between Playa Azul, Petatlán, and Acapulco (Azu-Aca). Four instruments, 5-10 km apart, were used at a total of 24 sites along the 320 km Pet-Mex profile, and 27 sites along the 180 km Azu-Aca profile. The Pet-Mex profile ended 50 km SW of Mexico City. The Azu-Aca

profile extended from Playa Azul (90 km NW of Petatlán), to Acapulco (Figures 1 and 3). Thirty-six aftershocks, located with the fixed local array, and well recorded over the Pet-Mex and the Azu-Aca moving arrays, were used as the equivalent of controlled seismic sources.

The main objective of this work is to use aftershocks of the Petatlán earthquake to define the structure of the Wadati-Benioff zone in the region. In addition we relate the 792 well recorded aftershocks to the seismic structure to better understand the rupture process of a major earthquake in the Mexican subduction zone.

PREVIOUS GEOPHYSICAL STUDIES ALONG THE MEXICAN SUBDUCTION ZONE

The results of geophysical experiments along the 1600 km of the Mexican Pacific coast are used to build a model for locating aftershocks in the Petatlán region. Shor and Fisher (1961) and Fisher (1961) used refraction profiles to determine the depth of the Mohorovicic discontinuity below the MAT. They profiled three sites within the Mexican portion of the MAT and provided the first shallow seismic model and reliable estimate of depth to the Moho discontinuity in that area. The Moho discontinuity was located between 9 and 16 km depth. Their profile, near Acapulco ran along the deepest portion of the trench, and is the closest to the area of interest of the present study. At this site, they determined an 8 km thick oceanic crust, with sediment and upper and lower crustal layers having P-wave velocities of 2.15, 5.25, and 6.82 km/ s, respectively.

On January 30, 1973, a earthquake occurred in the subduction zone off Colima, 350 km NW of Petatlán. Reyes *et al.* (1979) used offshore explosions to obtain travel time station corrections for locating the aftershocks of this earthquake. They used a flat layer crust with an upper mantle located at 30 km depth. The 50 aftershocks located with this model suggest two dipping planes, 15° and 30°. The former almost intersects the MAT. The ambiguity in the selection of the dipping plane is probably due to the small number of located aftershocks, and to the selection of a deep upper mantle for the region under the coast. A poorly-constrained P-wave fault plane solution for the main shock suggests a dipping fault plane of 30°.

Couch and Woodcock (1981) modeled gravity data for a profile 100 km SE of Acapulco, using an 8 km thick oceanic lithosphere following Shor and Fisher (1961).

Valdés *et al.* (1982) tested 25 modifications of Reyes seismic model on the arrival times of 30 Petatlán aftershocks, and used the model that produced the smallest origin-time residuals to locate 255 shocks of. Valdés *et al.* (1986) used offshore explosions recorded at inland seismic stations and offshore, and inland gravity data, to construct a two-dimensional seismic model for the ocean-to-continent transition in the state of Oaxaca, SW of the state of Guerrero. This model consisted of a continental, an accretionary, and an oceanic block, with an 8 km thick oceanic crust dipping 10° beneath the North America plate.

Simila *et al.* (1989), used explosions and earthquake data to refine and extend the model suggested by Valdés *et al.* (1986). LeFevre and McNally (1985) compiled focal mechanism data for 190 earthquakes associated with the subduction of the Cocos plate. The hypocenter locations (±30 km), and fault plane orientations from the focal mechanisms suggested a 10°-20° dip for the subducting oceanic plate north of the Tehuantepec Ridge (93°N), which is the region of interest in this study.

Two days after the 1985 Michoacán earthquake an aftershock occurred offshore adjacent to the Petatlán earthquake aftershock area. The P-wave fault plane solution indicated a thrust fault with a dip of 9°, smaller than the 14° obtained for the Petatlán event. The strike of the slip vector is N 39°E and N 26°E for the Michoacán main aftershock and for the Petatlán earthquake, respectively (Astiz, 1987; Chael and Stewart, 1982). Both directions are in agreement with the N33°±1°E slip vector projection for the Cocos-North America plates at 17.5°N and 101° W, using the NUVEL-1 model (DeMets and Stein, 1990).

The studies mentioned above suggest a shallow-dipping (10°) subduction zone NW of the Tehuantepec Ridge, with a trench at only 70-100 km from the coast. A flat layer seismic model in a shallow dipping subduction zone will introduce small (±4 km) location errors if the seismograph network is located directly above the aftershocks, and if the distance between stations (25 km in our case) is less than the hypocentral depth (Solte *et al.*, 1986; Bannister, 1988; Fuenzalida *et al.*, 1992; Comte *et al.*, 1992; Lindo *et al.*, 1992). Most of the Petatlán aftershocks, as will be shown later, are concentrated beneath the seismograph network at depths of less than 30 km; the remaining events are toward the coast, where an ocean bottom seismograph (OBS) was deployed. The locations of the remaining events are considered to be acceptable as they are within the largest distance between stations.

RESOLUTION OF THE NETWORK AND SEISMIC PARAMETERS

The seismic model used to locate the aftershocks of this study consists of 6 flat layers with constant velocities (Table 1). This velocity model was based on models from Colima (Reyes *et al.*, 1979), Petatlán (Valdés *et al.*, 1982, and 1986), and additional information from the previously mentioned studies. This flat layer model correlates closely with the depth-velocity distribution of the two dimensional subduction seismic model at a distance of 100 km from the MAT, which corresponds to the coast in the Petatlán area. The uppermost three layers of the model represent the Mesozoic intrusive granite, mapped by Ortega-Gutiérrez (1981). This granitic block extends 60 km inland, 25 and 75 Km north-west and south-east Petatlán. The three layers are intended to model the increase of velocity with depth, suggested by Valdés *et al.* (1986) for the Oaxaca area. The next two layers represent the oceanic crust, with velocities higher than typical (Spudich and Orcutt, 1980) due to the overburden pressure. The top of the oceanic crust is at a depth of 18 km at the shoreline in the area of Petatlán. The

top of the deepest layer is at a depth of 26 km, and represents the top of the upper mantle. Thus, the proposed model is a combination of continental and oceanic layers.

The hypocentral locations depend on P- and S-waves with good signal-to-noise ratio, the seismic -velocity model, and a well-distributed seismic recording network. The P- and S-wave arrivals were clear, but the network distribution was restricted by the Sierra Madre del Sur Range in one side and by the Pacific Ocean in the other. We tested the adequacy of the locator array. We use the computer program HYPOERROR, developed by Lienert *et al.* (1986). This program calculates the horizontal and vertical uncertainties in the location, as well as the time uncertainty in the origin time, for a geometrical distribution of the seismographic network and a velocity model. The program requires as input the seismic station distribution, a one dimensional velocity model, and the precision for selecting P- and S-wave arrival times. We calculated uncertainty maps for hypocentral parameters, at a depth of 30 km, with the seismic model defined in Table 1, using three seismic stations, and assuming typical reading errors of 0.05 and 0.10 sec for P and S waves, respectively. We found uncertainties of about 4 km in the location of these events.

Table 1

Z (Depth to top of layer, km)	Vp (km/s)	Vs (km/s)	σ Poisson's ratio	Layer
0.0	5.80	3.2	0.28	II
6.0	5.95	3.28	0.28	II
12.0	6.15	3.39	0.28	II
18.0	6.40	3.48	0.29	VI
24.0	7.05	3.83	0.29	VII
26.0	8.00	4.3	0.30	VIII

These errors correspond to the worst conditions during the Petatlán experiment. We used these conditions with HYPOERROR to calculate the uncertainties in the hypocenter location and the origin time, and compared them with the location errors given by the earthquake locator program. The calculated maximum horizontal and vertical error uncertainties for offshore events using the worst conditions are 7 and 5 km, respectively, and their uncertainty in origin time is 0.5 s, although realistically these errors may be larger. Resolution maps obtained by using more seismic stations and shallower depths provide

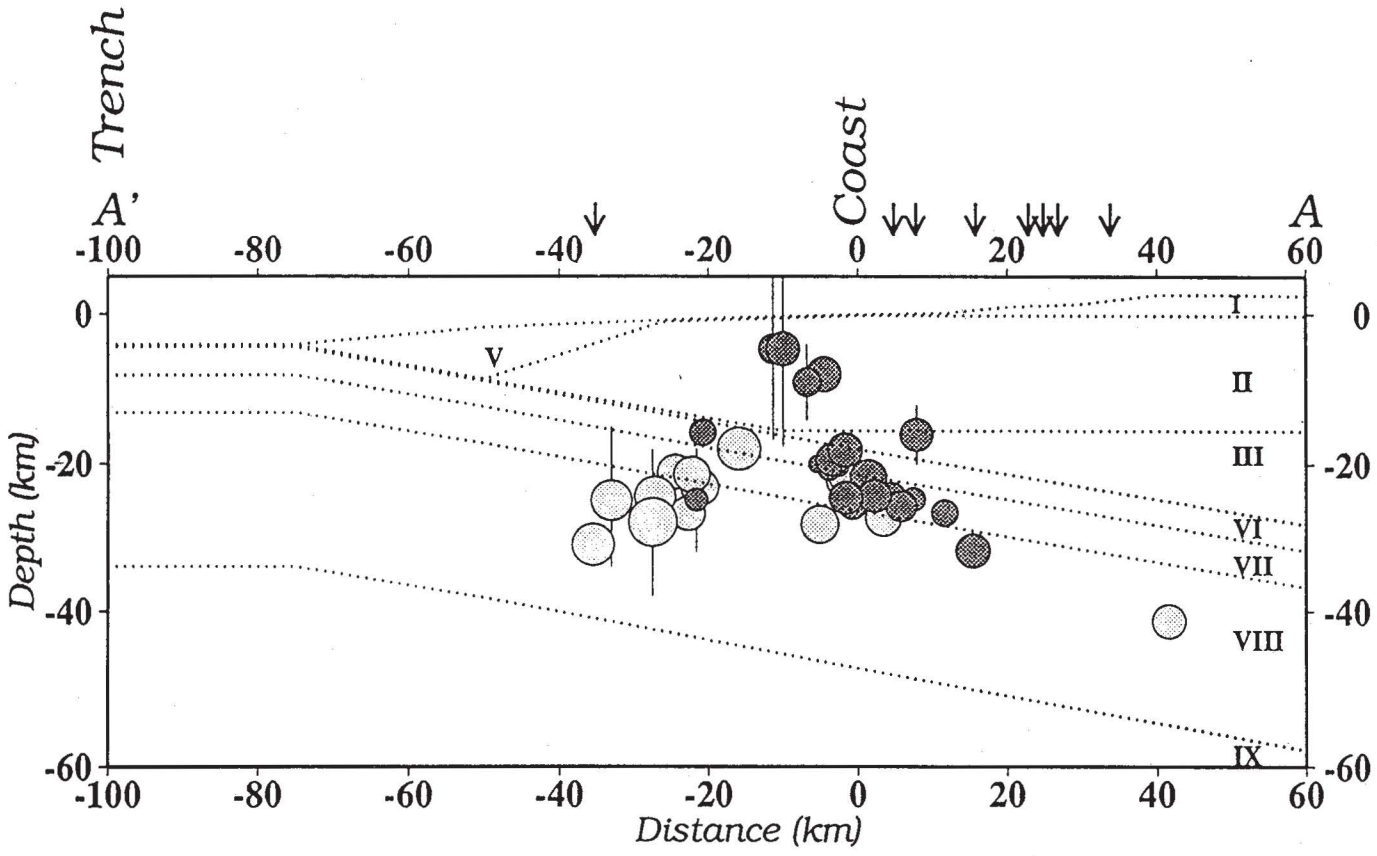

Fig. 2. Hypocenters of the 36 aftershocks from Figure 1, projected into a N 36°E vertical plane, roughly perpendicular to the Middle America trench in this region. Symbols are as in Figure 1. The arrows represent the seismographs. These aftershocks were used as controlled sources to model the ocean-to-continent transition along the subduction in this region. The bars centered at the hypocenters represent the standard vertical and horizontal errors in their location. The solid lines represent the final seismic model from Figure 9, and the Roman numerals correspond to the layers discussed in the text.

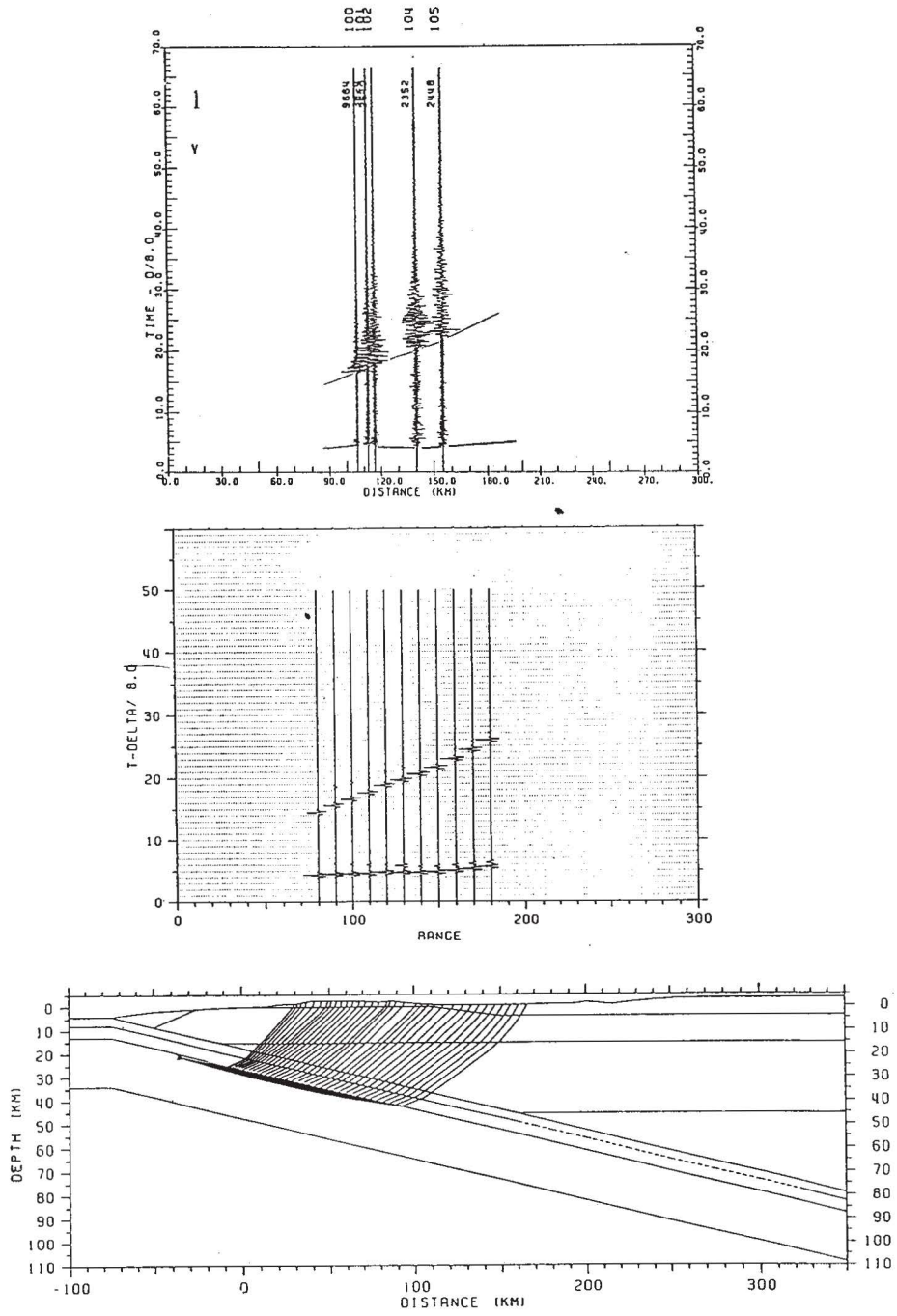

Fig. 3. Structural model (Bottom) and ray tracing for event 1 (Mc = 3.2), recorded at seismographs deployed between Petatlán and Mexico City, 60-100 km from the Pacific coast. The aftershock is located within the upper mantle, just below the oceanic crust at 21.1 km depth in the proposed model. The standard horizontal and vertical errors for this event are 1.7 and 1.1 km, respectively. The numbers in the model represent the different layers and are discussed in the text. Middle figure, synthetic seismograms calculated using the compressional-wave model, which correspond to the arrivals shown in the first 10 seconds, and synthetic seismograms calculated using the shear-wave model, which correspond to the arrivals after 10 seconds. Time is displayed as 8 km/s reduced time. Top, vertical seismic record section, arranged by epicentral distance, and shifted relative to origin time. The seismograms have been scaled relatively to their maximum amplitude (which is shown in counts, next to the traces) for a better display of the arrivals and also is an indication of the high dynamic range of the record. The numbers on top of the traces indicate the recording seismographs shown in Figure 1. The first arrivals for P- and S-waves correspond to direct rays from the lower oceanic crust. It can be seen, in both components, sharp P- and S-wave arrivals with no other clear seismic phases in between. The P- and S-waves have different frequencies, the latter being always lower as seen at seismograph 105. We observe an unusually large peak amplitude in the vertical component of seismograph 100, which is almost 3 to 4 times as large as the next and further away seismographs. The observed and the calculated P and S-wave arrival times are within 0.2 s. Stations 100-102 are located on the crystalline Range, Sierra Madre del Sur, while seismographs 104 and 105 are located in the boundary between this range and the Guerrero Basin.

smaller errors. We accept all earthquake locations that have location and origin time errors equal or smaller than the calculated by HYPOERROR. Valdés *et al.* (1982), found a 2.5 km horizontal and 4.5 km vertical shift in the location of 5 offshore Petatlán aftershocks when including the data from an OBS temporarily deployed offshore Petatlán and using the earthquake locator program HYPO71 (Lee and Valdés, 1985) with a flat layer seismic velocity model.

Nelson *et al.* (1989) relocated earthquakes from a study in the area of Oaxaca using the model for the subduction zone suggested by Valdés *et al* (1986). He found that the earthquakes were more accurately located by their program EQLOC than by HYPOINVERSE. The average event residual improved by 20% over the flat layered locations and the locations were more tightly constrained to the dipping slab, but computer memory requirements were 40 times greater for 3-D than for 1-D earthquake location algorithms.

The seismograms from the Petatlán aftershocks typically had a signal to noise ratio better than 10 to 1. The digital seismograms were displayed on a computer graphics terminal, and an electro-mechanical cursor was used to read the arrival times. The accuracy in reading the P- and S-wave arrival times from the digital seismograms was ±0.02 and ±0.05 seconds, respectively, based on reproducibility. The P- and S-wave arrival times from analog seismic records were read using a magnifying glass, and the accuracy was ±0.05 and ±0.10 seconds, respectively. The aftershock recording stations were located in a rectangular area of 32 km by 65 km, with the long axis parallel to the coast, and 55% of the aftershocks were directly below the recording array, at depths less than 30 km.

P- and S-wave phases were used to locate the aftershocks using the program HYPOCENTER (Lienert *et al.*, 1986) with the seismic model shown in Table 1. Smaller weighting factors were assigned to the analog P- and S-wave readings because of the lower reading accuracy. The program HYPOCENTER uses a damped least-squares solution (Crosson, 1976; Aki and Lee, 1976), which provides a more accurate location than HYPO71 (Lee and Valdés, 1985) or HYPOINVERSE (Klein, 1978), as it allows the solution to converge to a minimum by allowing the depth, latitude, and longitude to change, rather than fixing the depth. HYPOCENTER also uses centering and scaling, which are statistical regression procedures to improve the condition matrix which relates changes in arrival time to changes in hypocentral position.

The 36 aftershocks used as controlled sources have a mean RMS error of 0.27 sec in origin time, with a standard deviation of 0.17 sec. The average standard horizontal and vertical location errors, 2.9 and 5.7 km, respectively, are similar to or slightly larger than those predicted by the HYPOERROR program. We selected events with epicentral locations aligned with the profiling lines as much as possible, to minimize off the path profile errors. Figure 1 shows their epicentral locations. Figure 2 shows the aftershocks projected onto cross section A-A', which is approximately parallel to N 33°1° E, the convergence direction of the Cocos plate (DeMets and Stein, 1990). The magnitude of each event was calculated from coda duration from Lee *et al.* (1972). The magnitude range for these events is 1.6 to 4.4. Vertical and horizontal location errors are shown on Figure 2. Four events have large vertical errors (i.e. ERV≥ 18 km), but were still useful in the ray tracing procedure as it will be shown in the next section.

RAY TRACING

Hypocentral locations, origin times, and P- and S-wave arrival times from 36 selected events located by the local network, plus three or four stations in both profiling arrays, are used as controlled seismic sources to model the structure of the subduction zone in the areas between Petatlán and Mexico City, and between Playa Azul, Petatlán and Acapulco. We selected events that were recorded by as many stations along the profiles as possible. The hypocenters calculated from the local network are used as sources and the P- and S-wave travel times are computed from the observed P- and S-wave arrival times at the profiling seismographs, minus the calculated origin time. The horizontal components were rotated into radial and transverse components for easy identification of SH motion. The azimuth used for rotation was based on the earthquake locations. We used a ray-tracing algorithm (Luetgert, 1988) that implements a technique described by Cerveny *et al.* (1977) for calculating the propagation of rays through two-dimensional inhomogeneous media.

We assumed that the hypocenters and the seismographs lie on a plane. For the Pet-Mex profile the seismic stations are within 20 km of a vertical plane with a N 36°E strike. This direction is in agreement with the convergence direction of the Cocos Plate in this region (DeMets and Stein, 1990). The model is divided into quadrilaterals by layer interfaces and vertical grid lines. The velocity within each quadrilateral is interpolated from values at the four corners. Synthetic seismograms were obtained using the modified asymptotic ray theory by McMechan and Mooney (1980). In this algorithm, the waveform amplitude is determined by geometrical spreading and from plane-wave transmission and reflection coefficients along the ray path. A 1 Hz Ricker wavelet was used as the initial pulse for the calculation of synthetic seismograms.

The seismic model obtained for the state of Oaxaca (Valdés *et al.*, 1986) was used as the base model for the Petatlán area, as the hypocenters and fault plane solutions of large earthquakes (LeFevre and McNally, 1985) located in the 350 km between Petatlán and Oaxaca suggest a continuous Wadati-Benioff zone dipping 10°-15° to a depth of 80 km, with strike parallel to the coast (Figure 1). The Sierra Madre del Sur has been mapped as a continuous geomorphologic feature composed of crystalline and metamorphic rocks, with intrusives from the Precambrian, Paleozoic, Mesozoic, and in some cases from the Tertiary. Lopez-Ramos (1983) defines this 1110 km long and 120 km wide range as a continuous and well defined geological province.

A comparison of the geological and tectonic units traversed by both profiles (Oaxaca and Petatlán) shows that they intersect other ranges after they cross the Sierra Madre del Sur, which parallels the Pacific Coast. The Oaxaca profile intersects the Sierra de Juárez Range about 170 km from the Pacific coast. The geology of this range is complex. López-Ramos suggests that the sediments and metasediments on top of the Precambrian basement are allochthonous. The Pet-Mex profile intersects the Trans Mexican Volcanic Belt at about 200 km (Figure 1). Thus seismicity, topography and geology do not indicate major tectonic or structural changes in the area between Oaxaca and Petatlán, that may justify a significant change in the seismic model proposed for both regions.

For the present study a difference of ±0.5 s or less between computed and observed travel times was considered acceptable. This value comes from the accuracy in the determination of the origin time and hypocentral locations of the aftershocks, we cannot expect more accuracy in modeling the rays of the aftershocks than the accuracy in their location and origin time. Based on the Oaxaca model, several seismic models were tested. For each velocity model theoretical and observed travel times were compared for various phases. By refining the velocity-depth model in each trial, a satisfactory (<0.5 s) fit of the theoretical travel time curves to the observed data was achieved.

Amplitude modeling has been performed by trial and error, calculating the synthetic seismograms for realistic velocity-depth models and comparing their amplitudes and travel times with the observed data. The amplitude data helps constrain velocity gradients within layers. The profiles were not reversed, but the use of different hypocentral depths and record sections for similar stations, may be equivalent to reversing the profiles. The resolution and uniqueness of the two-dimensional models resulting from this forward, nonlinear modeling process are difficult to quantify. The sensitivity of the interpretation procedure was investigated by perturbing the interface position and the velocity gradients until the misfit between observed and calculated arrival times was less 0.5 s. In order to improve the fit between calculated and observed travel times, we varied the dipping angle between the oceanic and continental plates. Increasing the dip angle by one degree caused a misfit of 1.5 s between the observed and calculated travel times, and greater angles caused larger discrepancies.

The final model is structurally similar to the model from Oaxaca except that the distance between the trench and the Petatlán coast is 100 km, 25 km more than for the Oaxaca region. The models also differ in the location of the top of the oceanic crust under the coast, which is 11.5 and 17.6 km for the Oaxaca and Petatlán regions, respectively. The seismic velocities of the continental layers and the oceanic crust remain the same except for layer I (Figure 9), where it has been increased to account for the presence of the Sierra Madre del Sur and the volcanic range, consisting of thick andesitic materials (Campillo, 1989). We adopted the same accretionary block as in the Oaxaca model. The velocities of the upper mantle are 0.15 s slower compared to those of the Oaxaca model. Such a model produces theoretical travel times that are within 0.5 s of the observed ones. The objective of the present study is to define a two dimensional seismic structure in the area between Petatlán and Mexico City.

SHEAR WAVE VELOCITY MODEL

The shear wave model was derived from the compressional one by using a Vp to Vs ratio of 1.78, then adjusting the S-wave velocities in the model until the calculated shear wave arrivals were as close to the observed ones as possible. As in the case of the P-waves, the fit between observed and calculated arrivals was within the ±0.5 s estimated from the hypocenter location and origin time. Poisson's ratio was calculated from the P- and S-wave data sets modeled separately and then combined to give values for V_p/V_s. This procedure is intrinsically less accurate than by using the ratio of travel times in P- and S-waves between two reflectors, which would require near-normal incidence data. Poisson's ratio for the final model is 0.28± 0.03 in the continental block, increasing to 0.29±0.03 and 0.30±0.04 for the oceanic crust and the upper mantle, respectively.

RESULTS AND DISCUSSION

Figures 3 to 8 show the ray trace diagrams for selected aftershocks. The final model consists of continental, accretionary, and oceanic blocks, layers I-IV, V, and VI-IX (Figure 9), respectively. The accretionary block (Layer V, Figure 9) is the same as in the Oaxaca model. The layers that corresponds to the oceanic crust have velocities and thickness of 5.1-5.7 km/s and 3.5 km, 6.85-7.1 km/s and 5 km (VI and VII, Figure 9) and correspond to the basaltic and gabbroic layers. These velocities increase to 6.24 and 7.4 km/s when the oceanic crust reaches 40 km depth. This change in velocity was adopted from the Oaxaca model, where it was needed to fit the gravity and seismic data. Such an increase has been observed in other subduction zones (i.e. Lewis and Snydsman, 1979; Grow and Bowin, 1975) and may be explained as a phase change due to lithostatic pressure.

As no reflections or refractions have detected from the oceanic crust, it is constrained only by rays traversing it. The attitude of the oceanic crust is constrained by the sharp angle of the rays at the oceanic Moho, from a mostly horizontal to an upward path. A change of 1° (in the dip of the crust creates an arrival time misfit of 1.5 s. The upper mantle, below the oceanic crust (Layer VIII, Figure 9), with a velocity of 7.9-8.1 km/s, is well documented by most raypaths in the -40 to 100 km range. In some cases these rays sample the upper mantle down to 45 km depth (Figure 8). The Oaxaca model suggested a high velocity lid (IX ?, Figure 9), 21 km below the oceanic crust. The present data does not resolve this high velocity lid due to the interference of the coda waves with the direct arrivals. Layers I-III, (Figure 9) are sampled by rays traversing up–

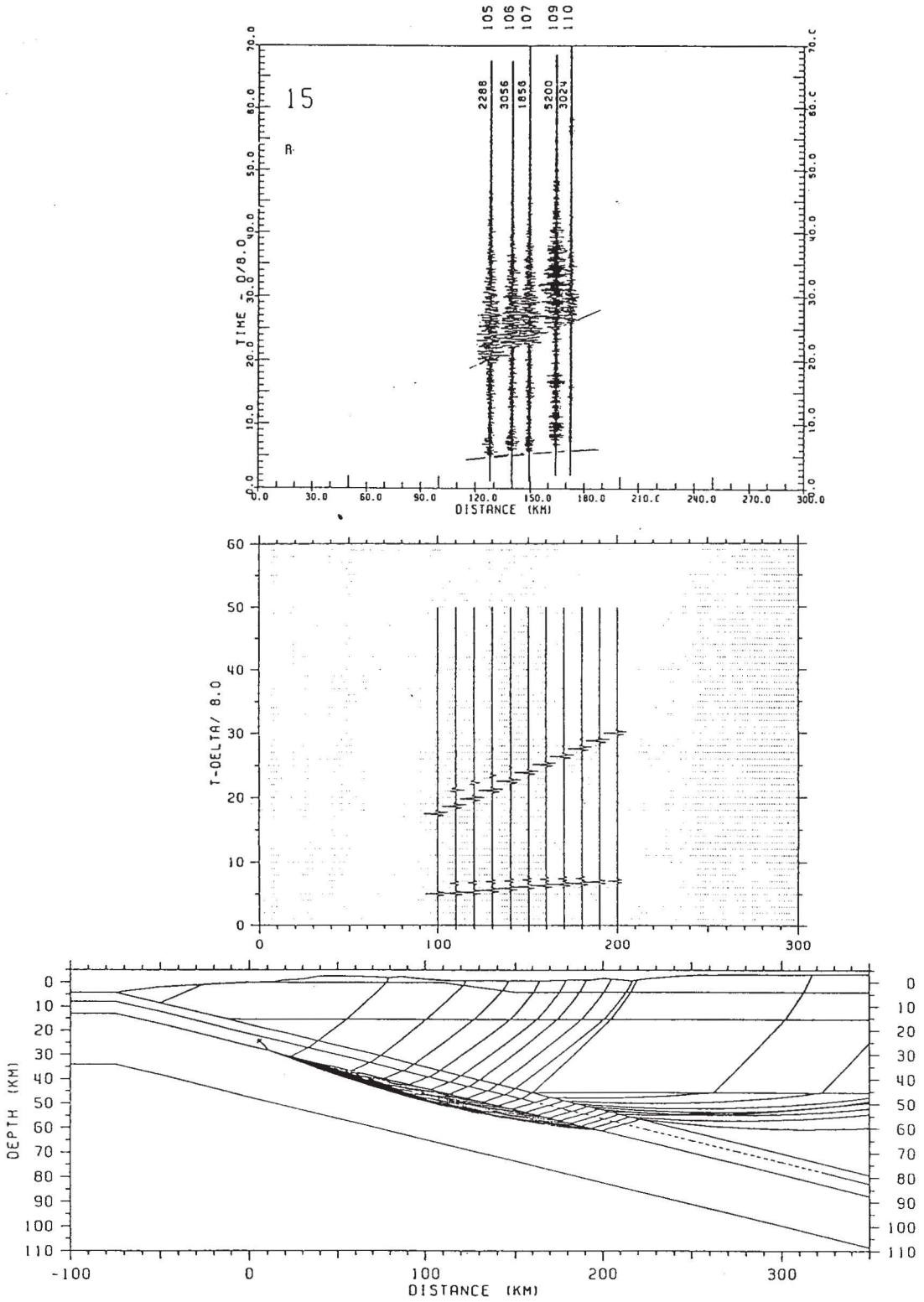

Fig. 4. Structural model (bottom) and ray tracing for event 3 (Mc = 2.9), recorded at seismographs deployed between Petatlán and Mexico City, 135-175 km from the Pacific coast. The aftershock is located within the oceanic crust, at 24.3 km depth and 5 km inland in the proposed model. The standard horizontal and vertical errors in this events location are 1.2 and 0.9 km, respectively. Symbols as in Figure 3. Radial component (top) is shown. The maximum P- and S-wave amplitudes for the vertical component, are very similar in this event. We also observe that the maximum amplitudes in the three components, slightly increase with distance for this event. The ray paths indicate that the seismic waves of this aftershock leave the oceanic crust, enter the oceanic upper mantle were they are refracted and move up again through the oceanic crust and into the continental crust. The synthetic and observed seismograms agree within 0.4 s.

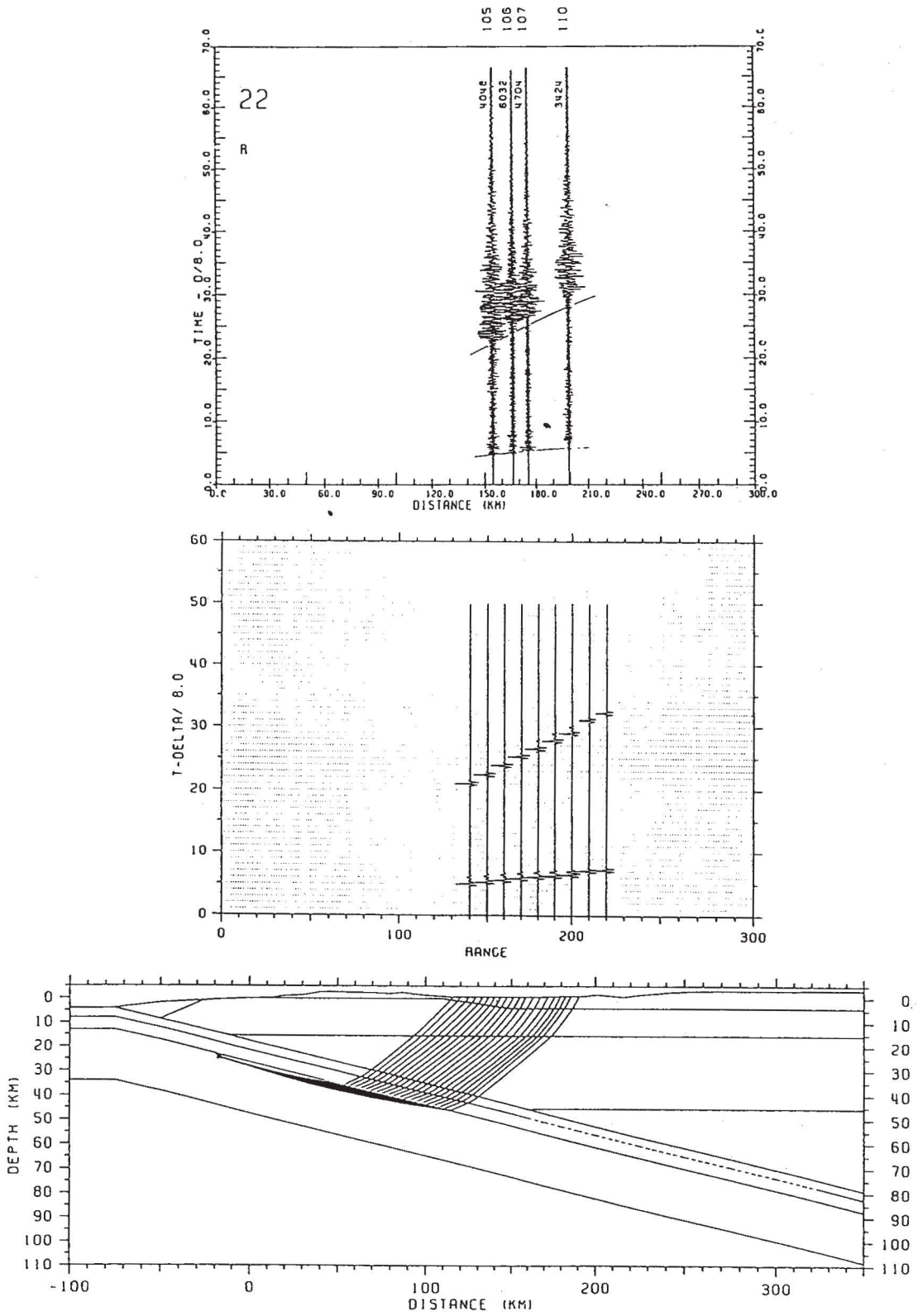

Fig. 5. Structural model (bottom) and ray tracing for event 6 (Mc = 3.7), recorded at seismographs deployed between Petatlán and Mexico City, 135-170 km from the Pacific coast. The aftershock is located below the oceanic crust, at 24.5 km depth and 20 km offshore of the coast in the proposed model. The standard horizontal and vertical location errors for this event are 2.6 and 5.6 km, respectively. Radial component (top) is shown. Symbols as in Figure 3. The ray paths from this event, are similar to those in Figure 3. Strong P-wave peak amplitudes comparable to those of S-wave are observed in the vertical component records. Clear S-wave arrivals are marked by a change in frequency. The observed P- and S-wave arrivals and those from the synthetic seismograms agree within 0.5 s.

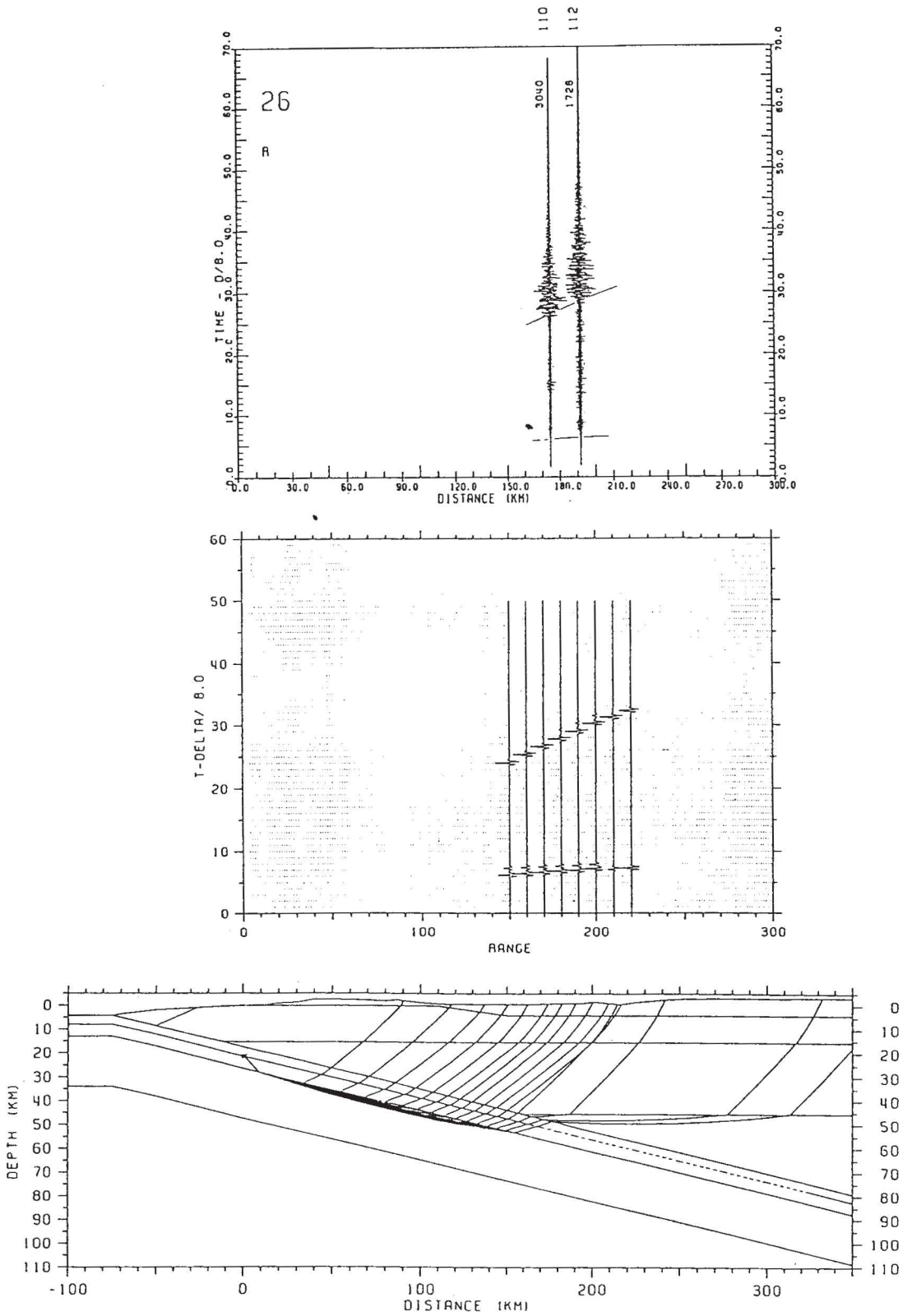

Fig. 6. Structural model (bottom) and ray tracing for event 7 (Mc = 3.6), recorded at seismographs deployed between Petatlán and Mexico City, 175-190 km from the Pacific coast. The aftershock is located within the oceanic crust, at 21.5 km depth and at the shore of the coast in the proposed model. Standard horizontal and vertical location errors for this event are 2.2 and 2.4 km, respectively. Radial component (top) is shown. Symbols as in Figure 3. The ray paths from this event are similar to those in Figure 4. P-wave peak amplitudes are small compared to those of S-wave as observed in the vertical component records (not shown). Clear S-wave arrivals have similar frequency content as P-waves (top). The observed P- and S-wave arrivals and those from the synthetic seismograms agree within 0.2 s.

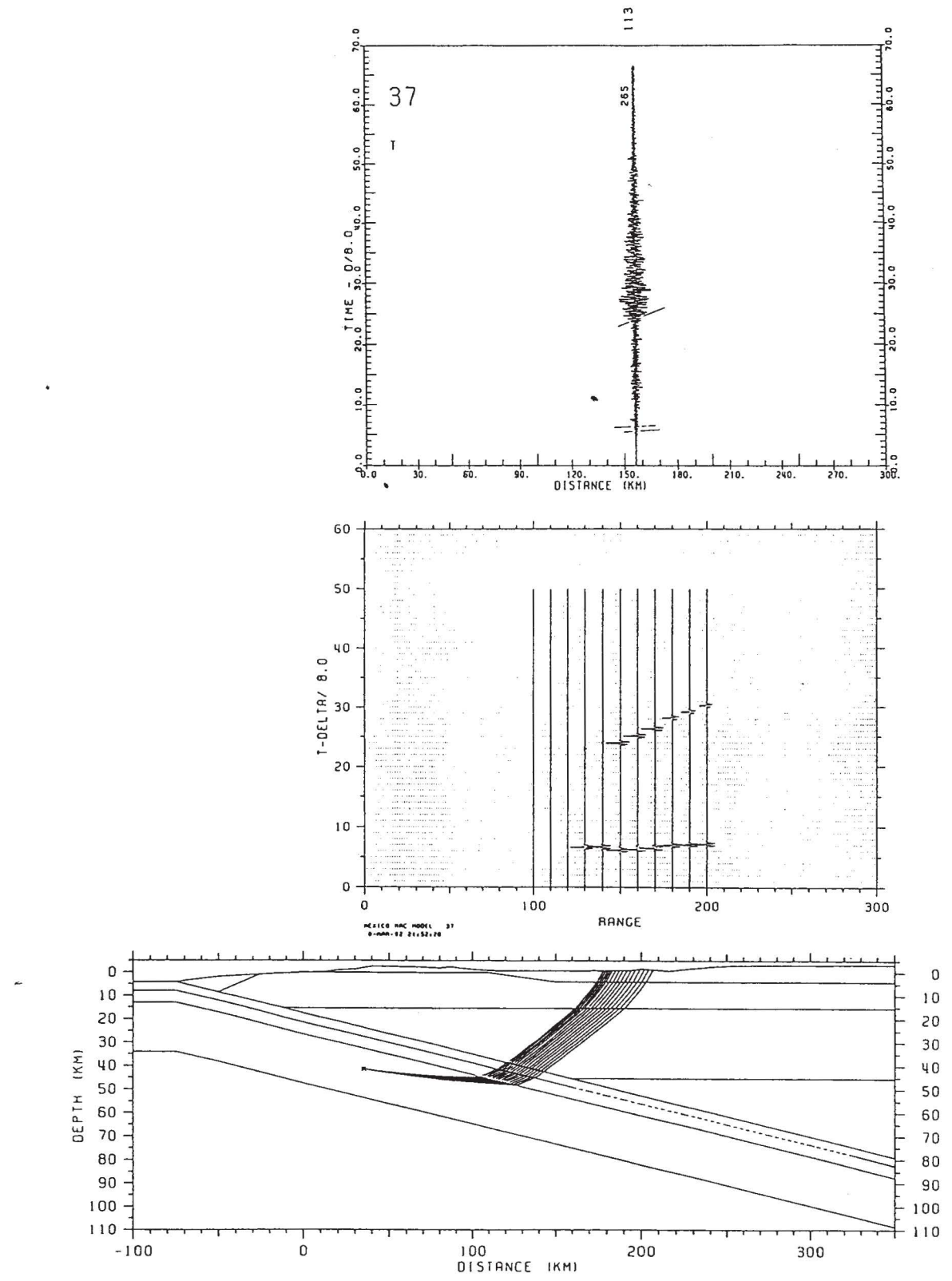

Fig. 7. Structural model (bottom) and ray tracing for event 9 (Mc = 3.0), recorded at a seismograph deployed between Petatlán and Mexico City, 195 km from the Pacific coast. The aftershock is located in the upper mantle below the oceanic crust, at 41.4 km depth and 35 km onshore of the coast in the proposed model. The standard horizontal and vertical location errors for this event are 1.8 and 1.2 km, respectively. Transverse component (top) is shown. Symbols as in Figure 3. The ray paths from this event are similar to those in Figure 3. P- and S-wave arrivals are not as clearly defined as in the previous Figures, probably due to its depth and small magnitude. The observed P- and S-wave arrivals and those from the synthetic seismograms agree within 0.5 s.

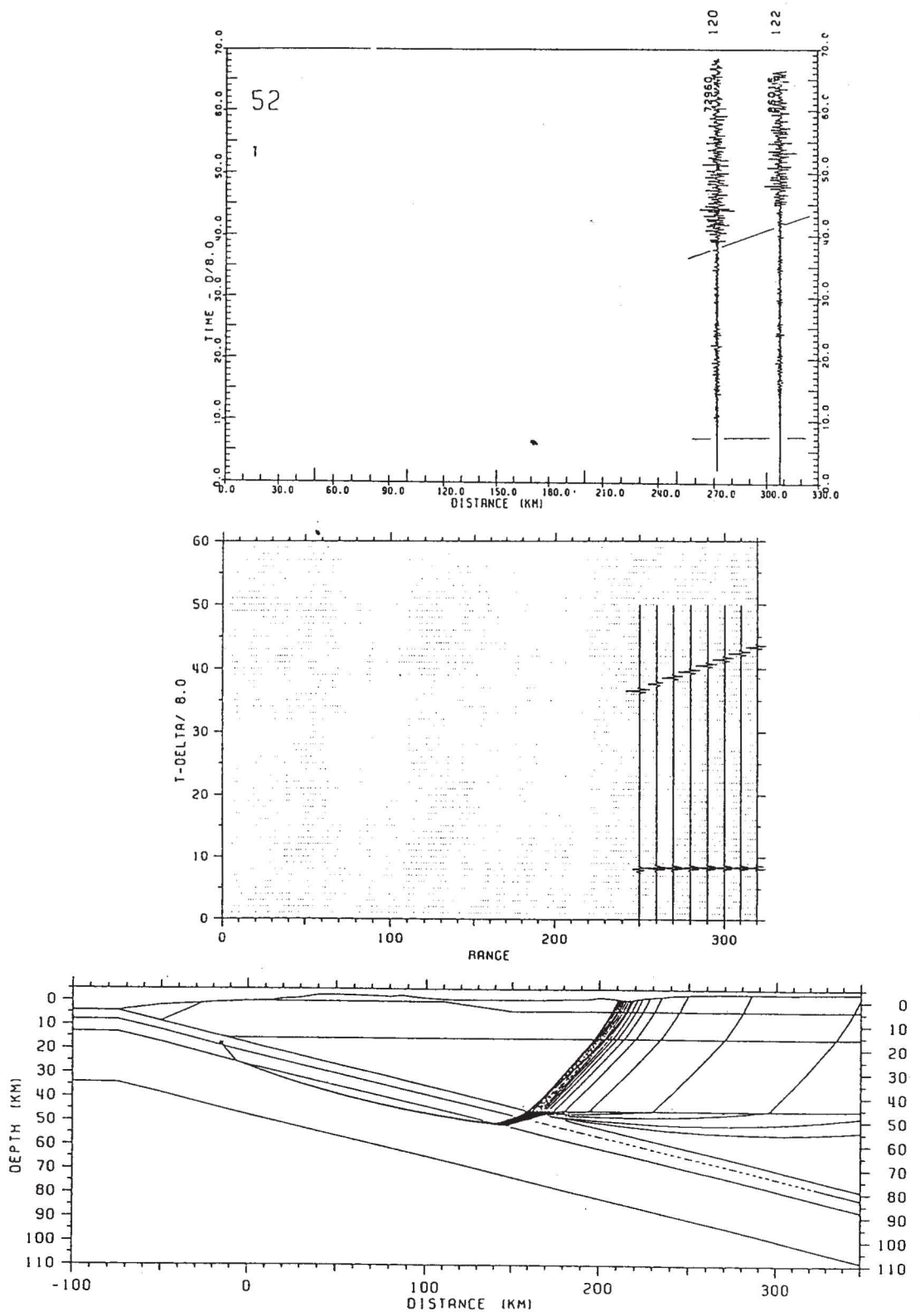

Fig. 8. Structural model (bottom) and ray tracing for event 12 (Mc = 3.9), recorded at seismographs deployed between Petatlán and Mexico City, 265-295 km from the Pacific coast. Station 120 and 122 are located in the Mexican Volcanic Belt. The aftershock is located within the oceanic crust, at 17.9 km depth and 15 km offshore of the coast in the proposed model. The standard horizontal and vertical location errors for this event are 4.5 and 6.0 km, respectively. This is the furthermost recorded event. Transverse component (top) is shown. Symbols as in Figure 3. The ray paths from this event are similar to those in Figure 4. The ray paths travel through the wedge of the lower continental crust. The P- and S-wave frequencies are lower compared to those of events recorded by seismographs closer to the coast. The observed P- and S-wave arrivals and those from the synthetic seismograms agree within 0.5 s.

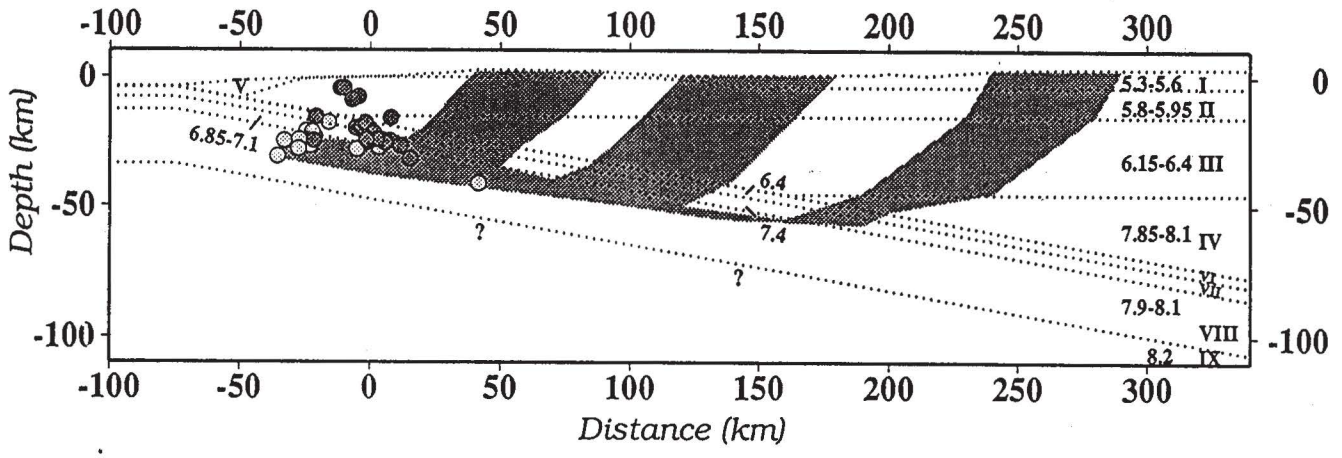

Fig. 9. Final model and composite of the travel paths (shaded area) from the events in Figures 3-8. Numbers correspond to different layers I-III to the continental crust layers, IV to the continental upper mantle, V to the accretionary layer, VI-VII to the oceanic crust, VIII represents the oceanic upper mantle, and IX (?) represents the oceanic lithosphere-asthenosphere boundary, which is suggested by the Oaxaca model, but not confirmed by our data. The shallow oceanic upper mantle in the -40 to 120 km range is well sampled by the ray paths. The oceanic crust is sampled at different ranges, 25-50, 80-140, and 170-200 km. The continental layers are sampled from 30-180 and 250-290. The oceanic crust is the structure where the seismic rays spent less time, but is important in controlling the turning angle of the rays. The dipping angle for the oceanic crust is 10°.

ward towards the surface. The continental block between 110 to 185 km range is sampled by a larger number of ray paths due to more aftershocks occurring at that time. The continental upper mantle (Layer IV, Figure 9) is sampled only by ray paths recorded at the more distant stations (Figure 3-8). This layer is poorly constrained by the data.

In general, first arrivals correspond to rays originating from within or below the oceanic crust. They travel in the upper mantle in a direction approximately perpendicular to the trench, where they are reflected. They cross the oceanic crust and transverse the layers forming the continental crust to the surface. The first arrivals for compressional and shear waves correspond to seismic waves refracted in the upper mantle. Figure 9 shows the regions sampled by the seismic rays. Between 40-60% of the paths are spent in the upper mantle, and the rest in the continental crust and (10% or less) in the oceanic crust. S-waves, in general, have lower frequencies than the P-waves (Figure 16), and the more distant seismograms have a lower frequency content. The observed seismic phases agree within 0.5 s with the synthetic travel times.

Pardo and Suárez (1995), based on accurately located hypocenters of local and teleseismic earthquakes, determined the shape of the Cocos Plate beneath the North America Plate in southern Mexico. They suggested that in the Guerrero region the subducted slab is subhorizontal. If we compare their model with the one obtained in this study, we observe that both models agree. Both predict a depth of 50 km for the top of the subducting slab at a distance of 250 km from the trench. All their hypocenters fall within the subducting oceanic crust of our model.

The model of the subducting lithosphere beneath Central Oaxaca, obtained by Valdés *et al* (1986), also agrees with section D of Pardo and Suárez (1995) and with the model presented here.

The data recorded along the strike of the Pacific coast (Azu-Pet-Aca profile) was modelled by the Pet-Mex model from where it intersects the Pacific coast. As the seismic sources and recording stations are closely aligned with the strike of the subduction zone, the resulting models have horizontal or gently dipping layers. The ray paths from the aftershocks in this profile, constrain the oceanic upper mantle between -30 and 25 km range. Figures 10 to 15 show the ray trace diagrams for events recorded in the Azu-Pet-Aca profile. The rays follow similar paths as those in the Pet-Mex profile. The first P- and S-wave arrivals of aftershocks located above or at the oceanic crust correspond to rays traveling upward for recording stations located at close range. Figures 10-13 show the seismograms recorded by stations 1-17, from Petatlán to Acapulco; Figures 14-15 correspond to seismograms recorded by stations 20-33 from Petatlán to Playa Azul. Stations 1-9, 23, and 30 are in Mesozoic intrusive granites and batholiths; stations 10-17, 20-22, and 32-33 in Paleozoic metamorphic rocks, and Station 30 is in Cenozoic intrusive rocks. No correlation was found between type of rock and amplitude or frequency content. The Azu-Pet-Aca profile provides a general two dimensional seismic model parallel to the MAT. The data are not suitable for a fine detail model.

Reduced Poisson's ratios were suggested for quartz-rich rocks in the continental crust at depths of 20-38 km (Luetgert, 1988). Our study shows lower Poisson's ratios for the continental crust rocks which correspond to the quartz-rich Xolapa Complex, while we observe higher Poisson's ratios for the oceanic crust and for the lower lithosphere.

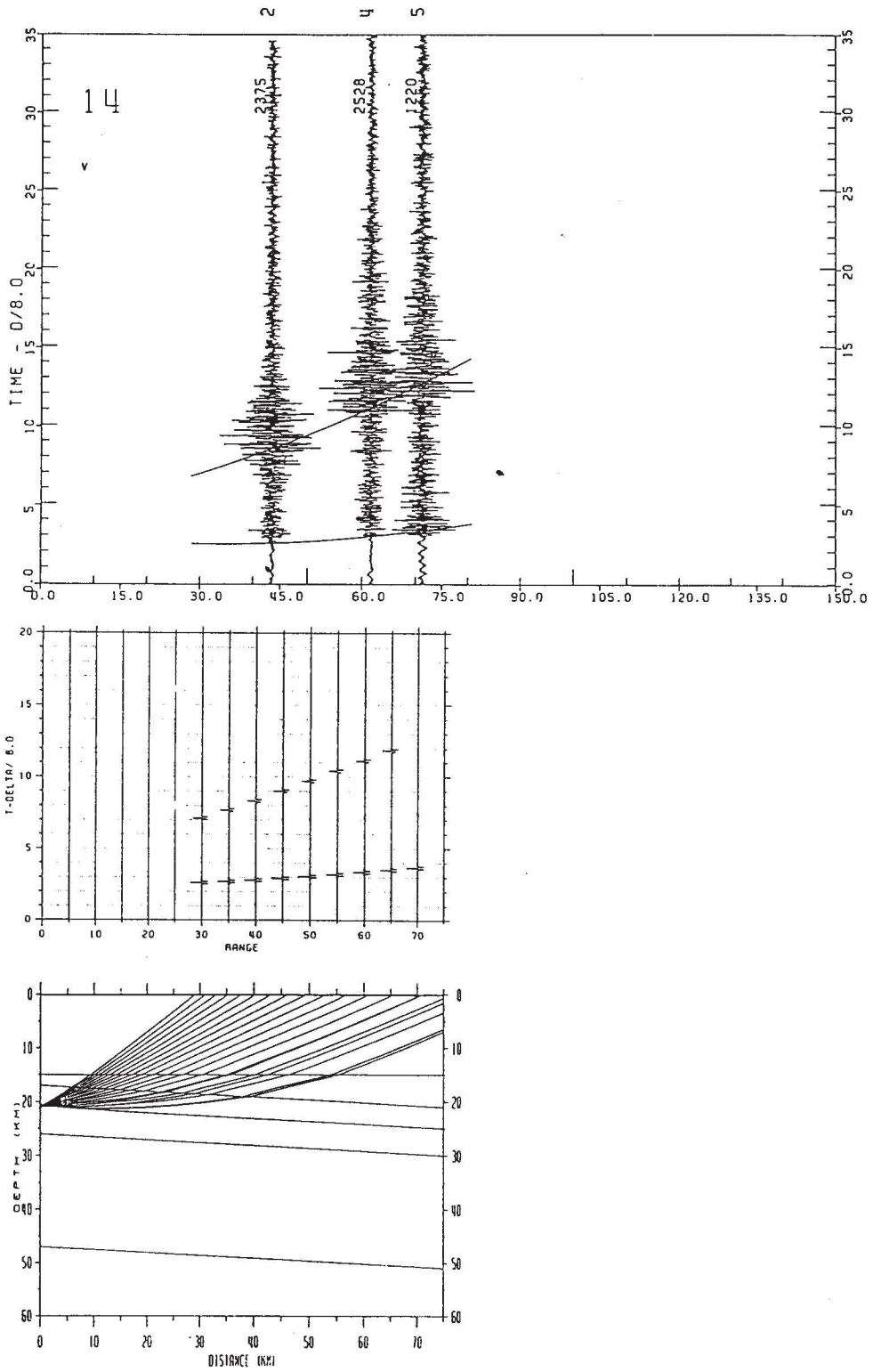

Fig. 10. Structural model (bottom) and ray tracing for event 14 (Mc = 2.0), recorded at seismographs deployed between Petatlán and Acapulco, approximately 45-72 km from Petatlán. The seismic model was obtained by projecting the subduction model defined in Figures 3-8 into a vertical plane containing the epicenter and the recording seismograph. The aftershock is located within the oceanic crust, at 20.8 km depth. The standard horizontal and vertical location errors for this event are 1.9 and 3.1 km, respectively Calculated synthetic seismograms (middle) and the Vertical component (top) are shown. Symbols as in Figure 3. The seismic ray paths from this event, travel upward through the oceanic crust, and reach the surface through the continental crust wedge. The most prominent arrivals in the observed records are those for the direct P- and S-waves. The observed direct P- and S-wave arrivals and those from the synthetic seismograms agree within 0.3 s. The peak amplitude decreases with distance in a similar ratio as for the event in Fig. 9, only by 1 % between seismographs 2 and 4 and by 50% between these seismographs and seismograph 5.

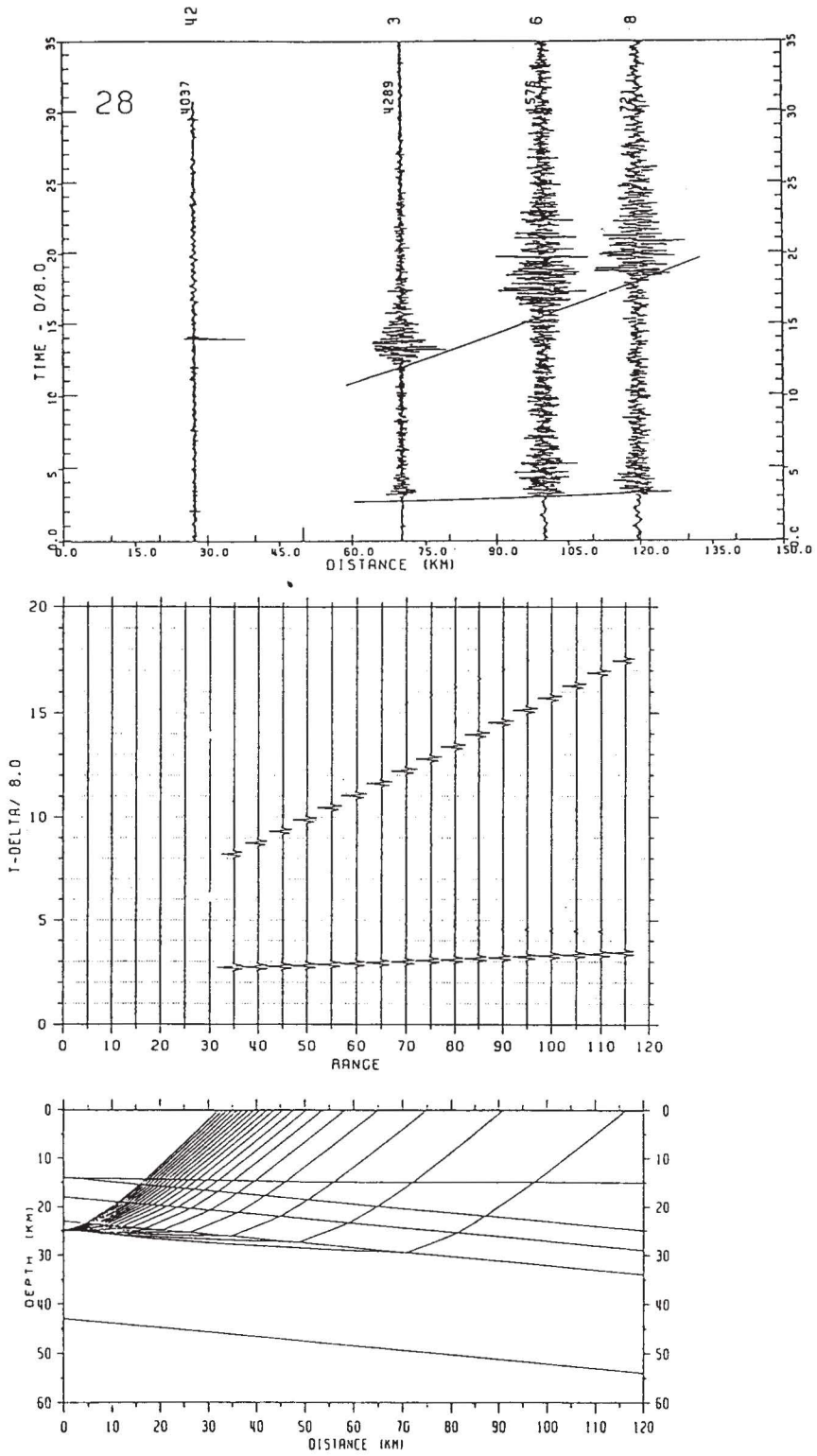

Fig. 11. Structural model (bottom) and ray tracing for event 16 (Mc = 2.1), recorded at seismographs deployed between Petatlán and Acapulco, approximately 70-120 km from Petatlán. The seismic model was obtained by projecting the subduction model defined in Figures 3-8 into a vertical plane containing the epicenter and the recording seismograph. The aftershock is located below the oceanic crust, at 24.9 km depth. The standard horizontal and vertical location errors for this event are 5.4 and 15.1 km, respectively. Calculated synthetic seismograms (middle) and the radial component (top) are shown. Symbols as in Figure 3. The seismic ray paths from this event, travel upward through the oceanic crust, and reach the surface through the continental crust wedge.The most prominent arrivals in the observed records are those for the direct P- and S-waves. The observed direct P- and S-wave arrivals and those from the synthetic seismograms agree within 0.3 s. The peak amplitude decreases with distance. At 30 and 50 km from Sta. 3, the peak amplitude of Stations 6, and 8, is 36 and 16 %, respectively.

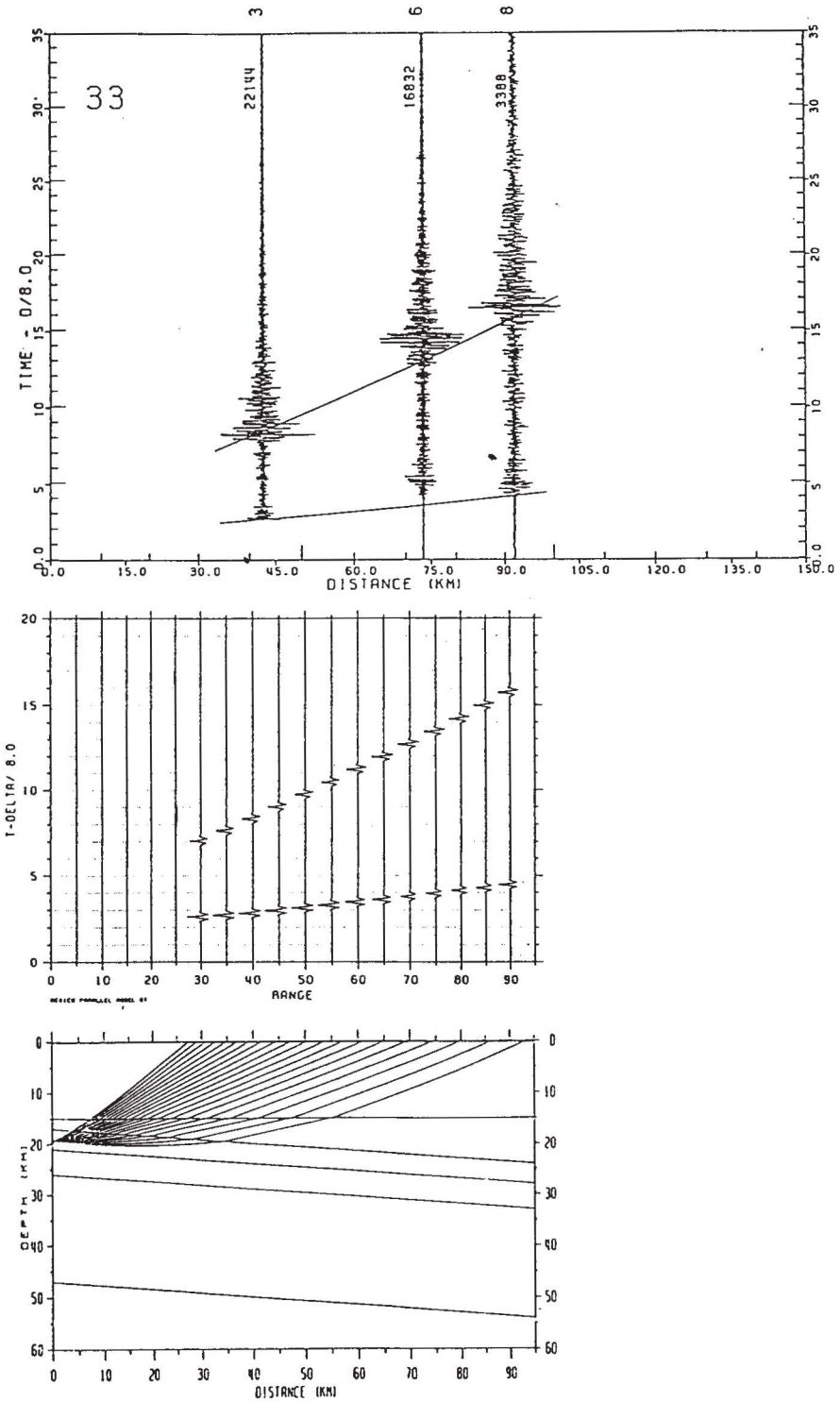

Fig. 12. Structural model (bottom) and ray tracing for event 18 (Mc = 3.0), recorded at seismographs deployed between Petatlán and Acapulco, approximately 40-90 km from Petatlán. The seismic model was obtained by projecting the subduction model defined in Figures 3-8 into a vertical plane containing the epicenter and the recording seismograph. The aftershock is located within the oceanic crust, at 19.4 km depth. The standard horizontal and vertical location errors for this event are 2.0 and 2.7 km, respectively. Calculated synthetic seismograms (middle) and the radial component (top) are shown. Symbols as in Figure 3. The seismic ray paths from this event, travel upward through the oceanic crust, and reach the surface through the continental crust wedge. Some of the rays traveling donward are reflected at the bottom of the oceanic crust. The most prominent arrivals in the observed records are those for the direct P- and S-waves, and are within 0.3 s of the calculated arrival times. The peak amplitude decreases with distance, and although Sta. 8 is 50 km further away than Sta. 3 with a peak amplitude 6 times smaller, the main P- and S-wave arrivals are clear.

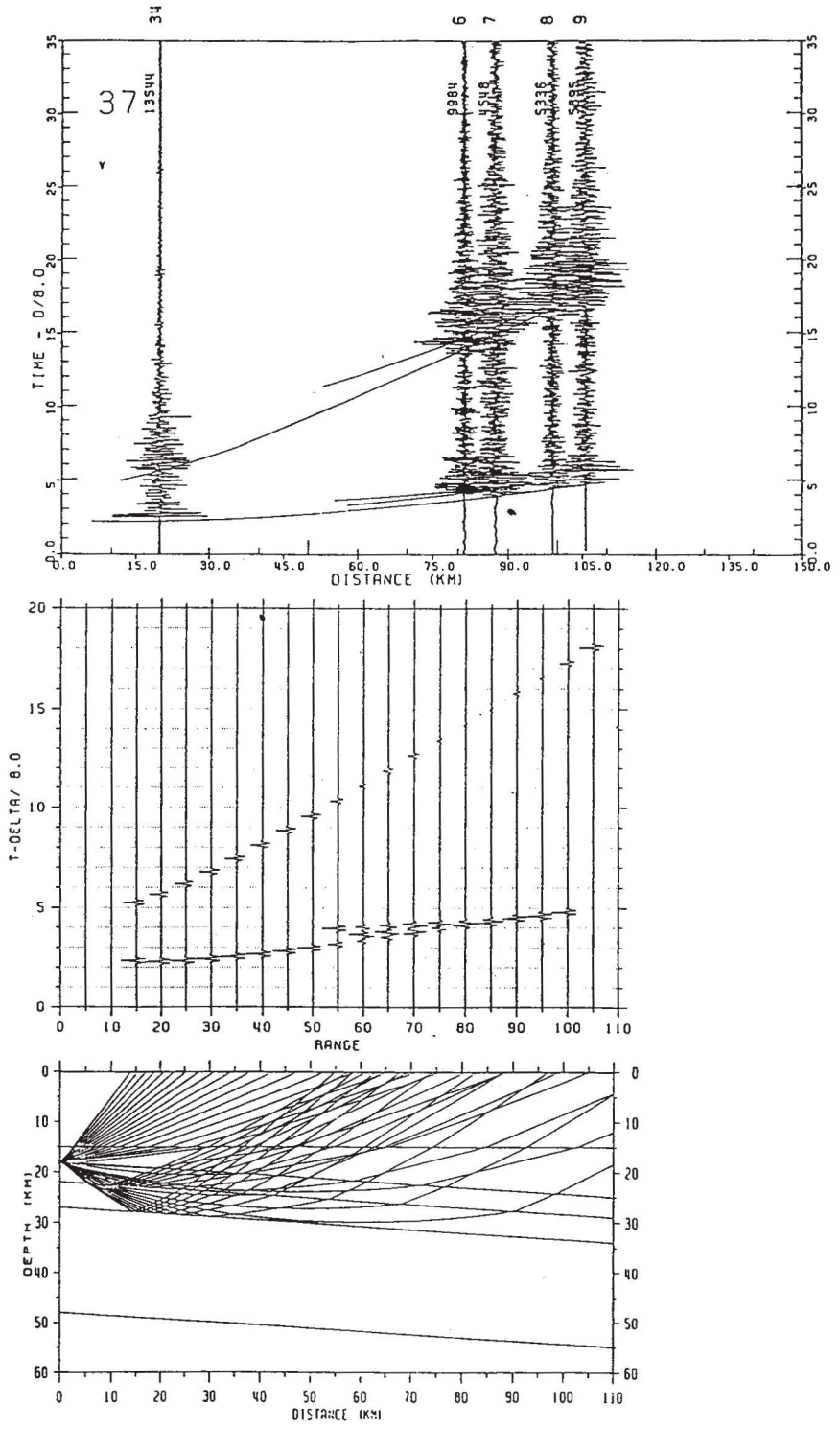

Fig. 13. Structural model (bottom) and ray tracing for event 20 (Mc = 3.1), recorded at seismographs deployed between Petatlán and Acapulco, approximately 20-105 km from Petatlán. The seismic model was obtained by projecting the subduction model defined in Figures 3-8 into a vertical plane containing the epicenter and the recording seismograph. The aftershock is located at the top of the oceanic crust, at 18.5 km depth. The standard horizontal and vertical location errors for this event are 3.0 and 3.8 km, respectively. Calculated synthetic seismograms (middle) and the vertical component (top) are shown. Symbols as in Figure 3. The seismic ray paths from this event, travel upward through the continental crust, and reach the surface. Some of the rays traveling donward are reflected in the layers of the oceanic crust. The complex P-wave arrival due to the reflections in the oceanic crust, is matched by the synthetic seismograms. The most prominent arrivals in the observed records are those for the direct P- and S-waves, and are within 0.4 s of the calculated arrival times. Following these direct arrivals are those from waves reflected in the oceanic crust. The peak amplitude decreases with distance between seismographs 34 and 7. Stations 8 and 9 have amplitudes slightly larger than seismo graph 7.

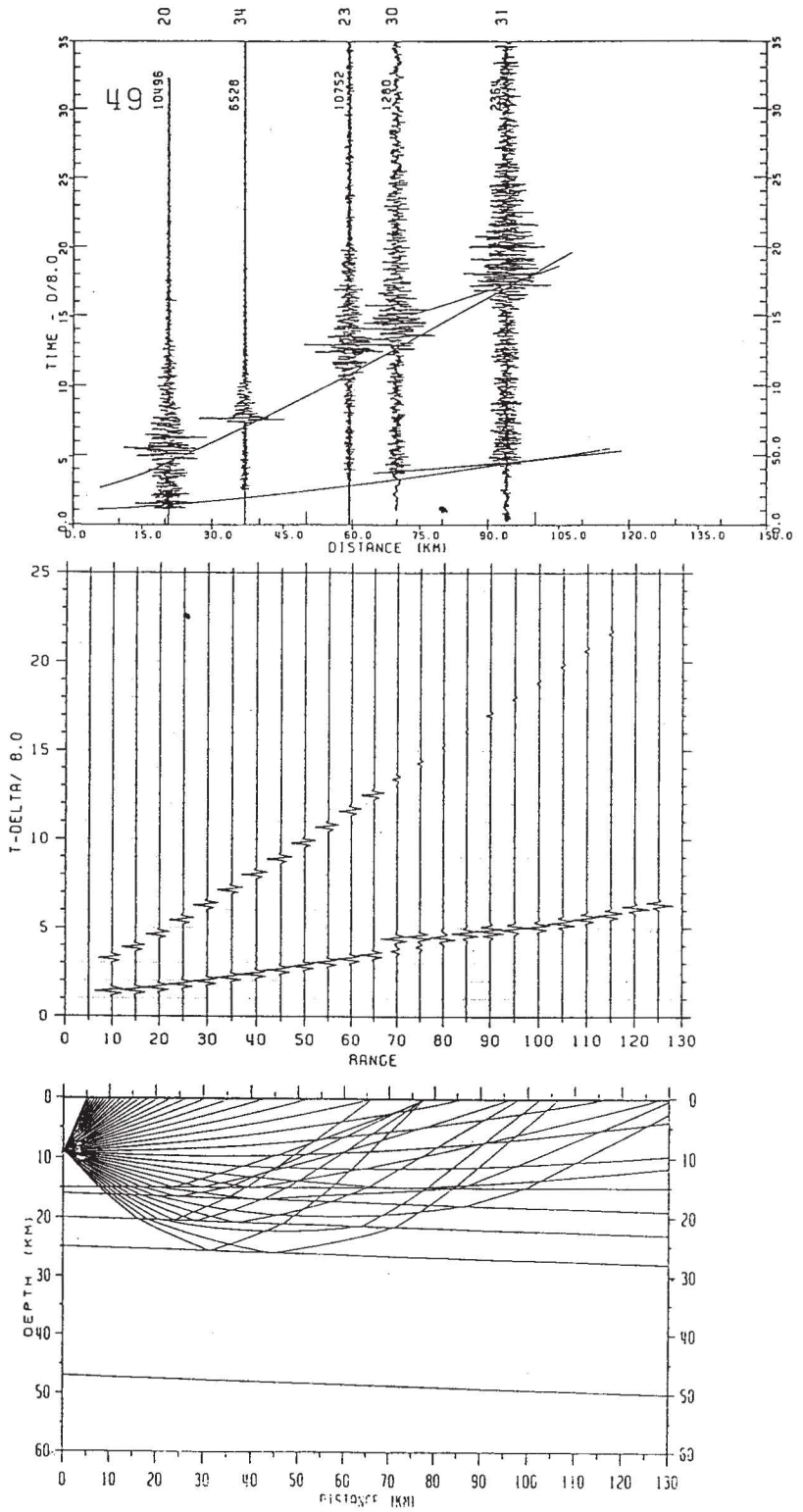

Fig. 14. Structural model (bottom) and ray tracing for event 24 (Mc = 2.5), recorded at seismographs deployed between Petatlán and Playa Azul, approximately 20-95 km from Petatlán. The seismic model was obtained by projecting the subduction model defined in Figures 3-8 into a vertical plane containing the epicenter and the recording seismograph. The aftershock is located within the continental wedge crust, at 9.0 km depth. The standard horizontal and vertical location errors for this events are 4.1 and 10.5 km, respectively. Calculated synthetic seismograms (middle) and the transverse component (top) are shown. Symbols as in Figure 3. The most prominent arrivals in the observed records are those for the direct P- and S-waves, and are within 0.4 s of the calculated arrival times. Reflected waves in the oceanic crust, arrive within 0.5 s of the direct arrivals in the 70 to 110 km range. The peak amplitude decreases with distance, although not uniformly. Seismograph 34 is located in the direction towards Acapulco, it has a very sharp S arrival and lower frequency content compared to the other seismographs in the opposite direction.

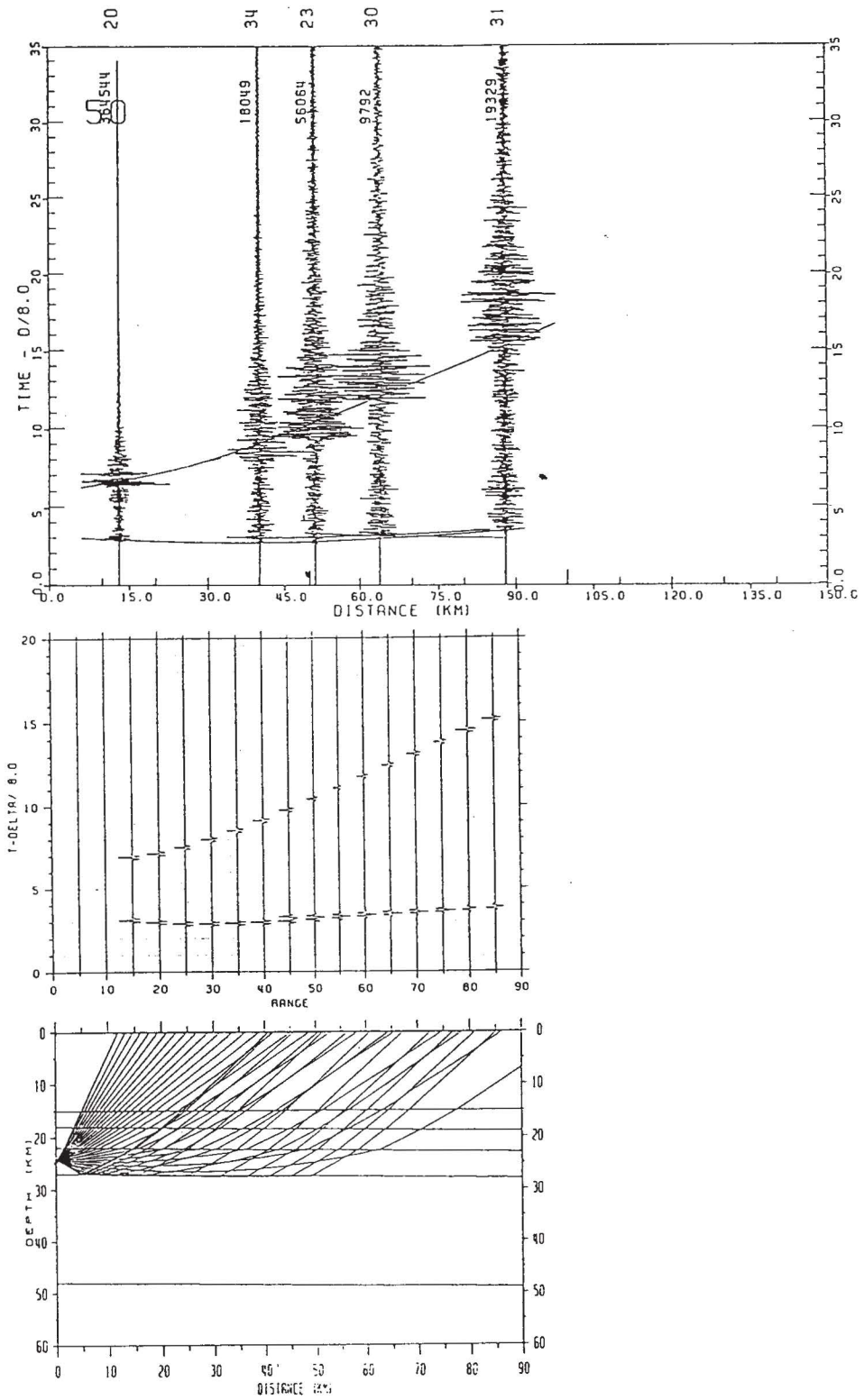

Fig. 15. Structural model (bottom) and ray tracing for event 25 (Mc = 3.0), recorded at seismographs deployed between Petatlán and Playa Azul, approximately 15-90 km from Petatlán. The seismic model was obtained by projecting the subduction model defined in Figures 3-8 into a vertical plane containing the epicenter and the recording seismograph. The aftershock is located within the oceanic crust, at 24.5 km depth. The standard horizontal and vertical location errors for this event are 2.7 and 2.4 km, respectively. Calculated synthetic seismograms (middle) and the transverse component (top) are shown. Symbols as in Figure 3. The most prominent arrivals in the observed records are those for the direct P- and S-waves, and are within 0.3 s of the calculated arrival times. Reflected waves in the oceanic crust, arrive within 0.5 s of the direct arrivals in the 40 to 85 km range. The peak amplitude decreases with distance, except for seismographs 23 and 31.

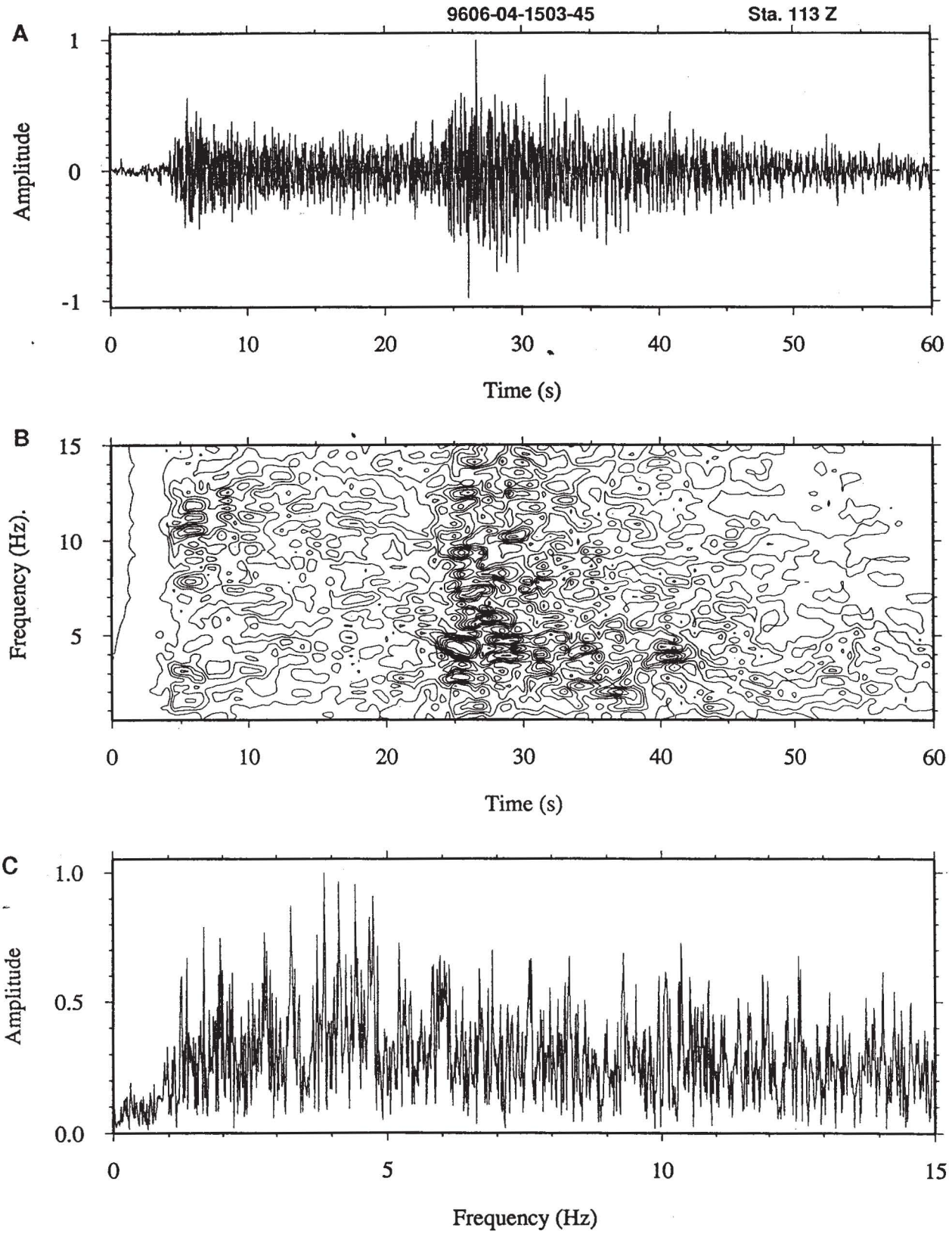

Fig. 16. (A) Seismogram of an event recorded on station 113 in the vertical component. P-wave arrival starts at about 4 s, and from its peridogram (B) we observe its characteristic frequency of about 3 Hz, followed by arrivals with 8 and 12 Hz, but also some energy at about 3 Hz. The S-wave arrival is at about 24 s. with a characteristic frequency of 5 Hz, also followed by higher frequency, 6 to 12 Hz, arrivals. This type of analysis helped us to identify the arrivals. The power spectrum of the whole record is also shown (C).

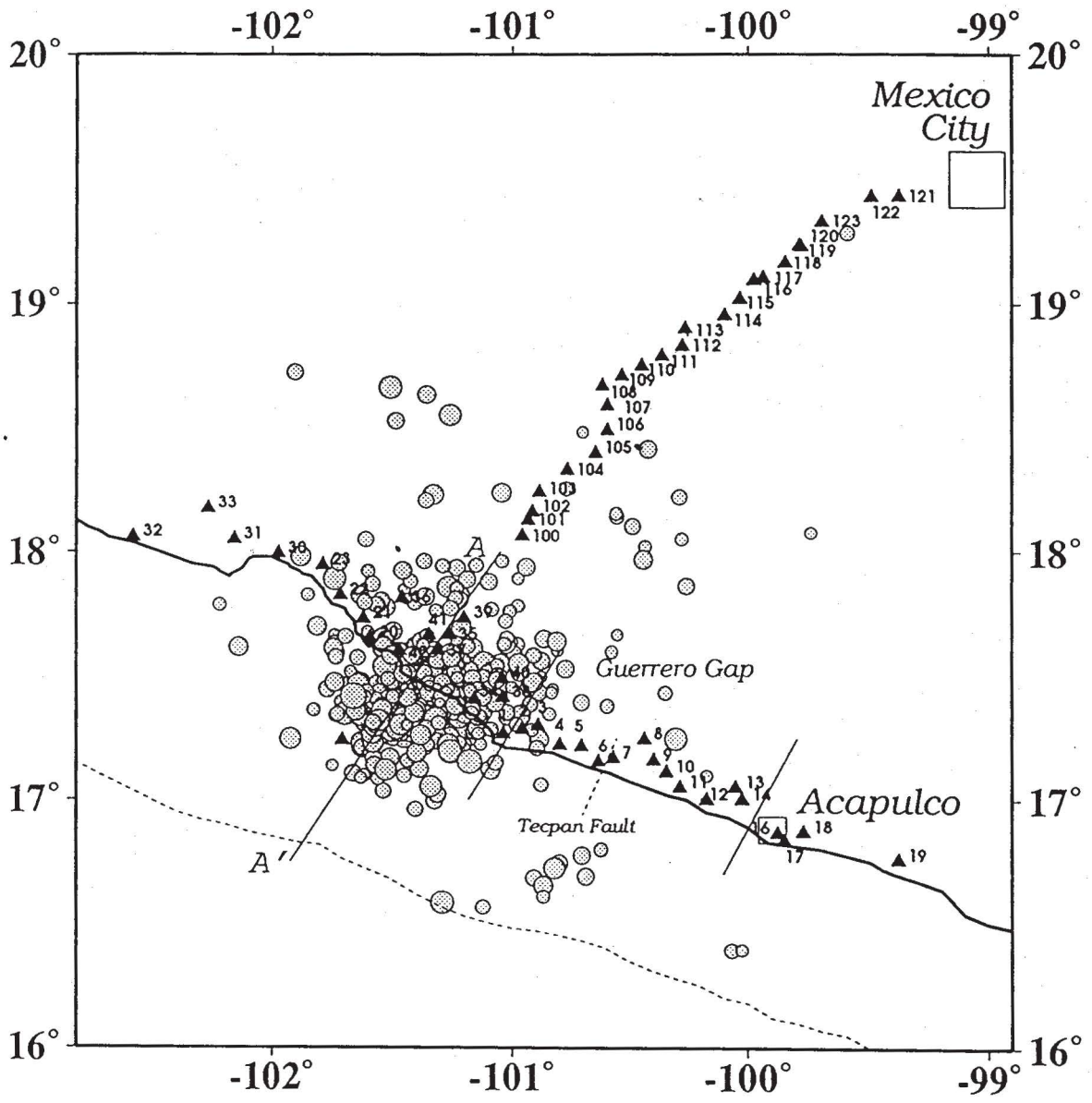

Fig. 17. Epicentral locations (circles) of 591 Petatlán earthquake aftershocks with RMS origin time smaller than 0.5 s, recorded during one month. Triangles are seismographs of the Pet-Mex, Pet-Aca, and Pet-Azu profiles. The locating network is obscured by the aftershock epicenters. Cross section A-A' is shown in Figure 9. The dashed line represents the Tecpan Regional Fault (Sandoval, 1985). A cluster of 7 earthquakes is located at the SW end of the fault. The Tecpan fault and the location of this cluster, correlate with a bathymetric in that region (Fisher 1961). The Tecpan fault may represent a zone of weakness in this gap. Solid lines represent the boundaries of the Central Guerrero seismic gap, defined to the West by the extent of the Petatlán aftershock area, and to the East by the 1957 (Ms~ 7.7), Acapulco earthquake.

Figures 3 and 14 show the ray paths of two Petatlán aftershocks toward Mexico City and Acapulco, respectively. The events have hypocenters at about 21 km depth and magnitudes of 3.2 and 3.3. Despite similarities, and although the seismic model toward Mexico City is structurally more complicated than toward Acapulco, the P- and S-wave are more impulsive and clear in the Pet-Mex profile than the Pet-Aca. The coda-wave seismic attenuation profile is 10-40% higher along the coast than toward Mexico City (Valdés-González, 1993, using the same events as in this study). Christensen (1984) showed a preferred alignment direction for olivine and pyroxene in ophiolites from several locations, and predicted P-wave anisotropy of 3 to 8 percent for the oceanic upper mantle. The fast direction was found to be perpendicular to the fossil spreading direction. The Pet-Mex profile is orthogonal to the motion vector projection of the Cocos plate. Thus the fact that seismic waves of coastal earthquakes propagating perpendicular to the trench reach further distances than waves propagating along the coast can be attributed to the

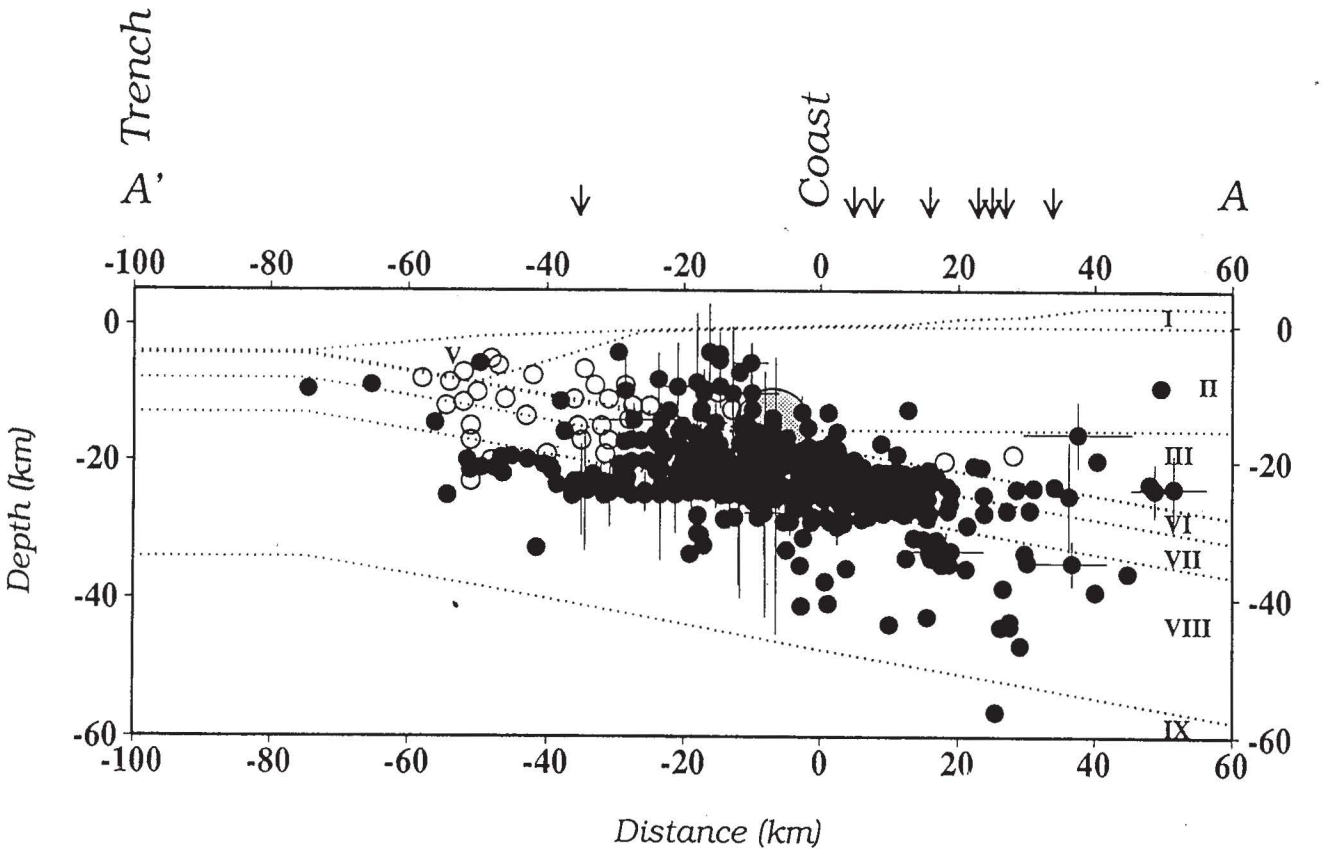

Fig. 18. Cross section along A-A' from Figure 17 showing the 591 hypocenters (solid circles). Horizontal and vertical standard errors greater than 5 km in the hypocentral location are indicated with bars. Dotted lines represent the two-dimensional seismic model from Fig. 9. Arrows represent the locating seismographs. The location of the main shock (large circle) was obtained using a portable seismic network deployed within 150 km of the epicenter (Gettrust *et al*, 1981). The Petatlán earthquake is located in the boundary between the oceanic plate and the continental plate in our model. Eighty five percent of the aftershocks are located in the oceanic crust, 3 percent above, and 12 percent below it. There is a concentration of Petatlán aftershocks downdip, further away from the trench. These site corresponds to the location of an asperity (Valdés *et al.*, 1982; Hsu *et al.*, 1984; and Astiz, 1987). The aftershocks define a narrow Wadati-Benioff zone, which agrees with the proposed seismic model. The updip segment of the oceanic crust (-30 to -70 km), devoid of aftershocks, was later occupied by the location of the aftershocks (open circles) of the Ms~ 7.5 aftershock of the 1985 Michoacán earthquake. The size of the aftershocks for both earthquakes is constant regardless of their magnitude, to more accurately compare their relative location.

two dimensional velocity structure as well as to lower seismic attenuation in the general direction perpendicular to the trench due to anisotropy.

SEISMIC MODEL AND AFTERSHOCK LOCATION

We have located 792 Petatlán aftershocks using the model from Table I. These events were well recorded by 4 or more of the stations deployed in the aftershock area, and have signal to noise ratios of at least 10 to 1 for the P-waves. RMS errors of time residuals were calculated for each event, and the overall mean average RMS is 0.15 s with a standard deviation of ± 0.09 s. Figure 17 shows the epicentral distribution of 591 events with RMS time residuals less than 0.5 s. These events cluster in an ellipsoid with 90 by 60 km axes. The long axis is roughly parallel to the MAT. Figure 18 shows the hypocentral locations of these 591 events projected onto the cross section A-A', perpendicular to the trench. At least 85 percent of the aftershocks are located in the oceanic crust, 3 percent above the oceanic crust, and the remaining 12 percent below the oceanic crust. In cross section the aftershocks are clustered in a section 50 km long, which extends from 30 km offshore to 20 km inland, and from 20 to 30 km depth (Figure 18). The location of the main shock (Gettrust *et al.*, 1981) is at the top of the crust and near the center of the aftershock section. There is a concentration of seismic activity at the deeper end of the oceanic crust section while near the trench the activity is scarce. The area of greatest activity may be an asperity (Valdés *et al.*, 1982; Hsu *et al.*, 1984) based on the distribution of foreshocks and aftershocks and the amount of energy release per unit area according to Bath (1979). The concentration of activity is in an area where strong coupling can occur, as the young oceanic lithosphere is being subducted at a high convergence rate (Astiz, 1987; McNally *et al.*, 1986). Preliminary calculations of fault slip distribution during the Petatlán earthquake (Mendoza, personal communication), suggest that the area of high aftershock concentration is

located 20 km North and updip from the area with the maximum slip (77 cm); however, it is still located in a region of large slip (55-60 cm).

CONCLUSIONS

We have modeled the compressional- and shear-wave velocity structure of the ocean-to-continent transition in the state of Guerrero, southern Mexico, using well located aftershocks recorded by temporary stations deployed between the Pacific coast and Mexico City and between Petatlán and Acapulco. The data suggest an 8 km thick oceanic crust that dips 10° in a direction N 36° approximately perpendicular to the Middle America Trench.

The seismic rays originating offshore and under the oceanic crust reach Mexico City by traveling along the oceanic lithosphere for up to 200 km, then crossing the subducted oceanic crust and gradually steepening their path as they travel through continental crustal layers. Seismic waves of coastal earthquakes ($M_c \leq 4$) propagating perpendicular to the trench, are observed at further epicentral distances than waves from the same earthquakes propagating along the coast, due to the two-dimensional seismic structure in the direction perpendicular to the trench (shallow dipping angle), and velocities that increase with depth in the oceanic and continental blocks as well as the low seismic attenuation in that direction (Valdés-González, 1993).

Eighty-five percent of the 792 Petatlán earthquake aftershocks are located within the oceanic crust, defining a thin Wadati-Benioff structure. There is a concentration of events, with hypocenters located deeper and further away from the trench, in an area previously defined as an asperity by using Petatlán aftershocks. The shallower, updip segment of oceanic plate devoid of Petatlán aftershocks was filled by aftershocks of the September 19, 1985 main aftershock ($M_S = 7.5$, Zihuatanejo earthquake). The occurrence of aftershocks, both down- and up-dip on this segment of the oceanic plate, suggests that the Petatlán segment has now fully ruptured but only after producing two large earthquakes M_s (7.5-7.6) within 6.5 years.

ACKNOWLEDGMENTS

We would like to thank many people that helped during the data gathering, including: William Unger, Lee Powell, Wayne Penington, Robert Meyer and Hans Meyer, and: Jim Luetger and Bruce Karsh for data processing. Cinna Lomnitz and two anonymous reviewers provided valuable comments.

BIBLIOGRAPHY

AKI, K. and W. H. K. LEE, 1976. Determination of three-dimensional velocity anomalies under a seismic array using first P arrivals times from local earthquakes. I. A homogeneous initial model. *J. Geophys. Res., 81*, 4381-4399.

ASTIZ, L., 1987. I Source analysis of large earthquakes in Mexico, II Study of intermediate depth earthquakes and interplate seismic coupling. Ph. D. Thesis, California Institute of Technology.

BANISTER, S., 1988. Microseismicity and velocity structure in the Hawkes Bay Region, New Zealand: fine structure of the subducting Pacific Plate. *Geophysical J. 95*, 45-62.

BATH, M., 1979. Introduction to Seismology, 488 pp., Birkhauser Verlag, Boston, Mass.

CERVENY, V., I. A. MOLOTKOV and I. PSENCIK, 1977. Ray Method in Seismology, Univerzita Karlova, Praka, Czechoslovakia, 214 pp.

CAMPILLO, M., J. C. GARIEL, K. AKI and F. J. SANCHEZ-SESMA, 1989. Destructive strong ground motion in Mexico City; Source, path and site effects during great 1985 Michoacán earthquake. *Bull. Seism. Soc. Am., 79*, 1718-1735.

CHAEL, E. P. and G. S. STEWART, 1982. Recent large earthquakes along the Middle American trench and their implications for the subduction process. *J. Geophys. Res., 87* (B1), 329-338.

CHRISTENSEN, N. I., 1984. The magnitude, symmetry and origin of upper mantle anisotropy based on fabric analyses of ultramafic tectonites. *Geophys. J. R. Astron. Soc., 76*, 89-111.

COMTE, D., M. PARDO, L. DORBATH, C. DORBATH, H. HAESSLER, L. RIVERA, A. CISTERNAS and L. PONCE, 1992. Crustal seismicity and subduction morphology around Antofagasta, Chile: preliminary results from a microearthquake survey. *Tectonophysics, 205*, 13-22.

COUCH, R. and S. WOODCOCK, 1981. Gravity and structure of the continental margins of southwestern Mexico and northwestern Guatemala. *J. Geophys. Res., 86*, 1829-1840.

CROSSON, R., 1976. Simultaneous least squares estimation of hypocenter and velocity parameters. *J. Geophys. Res., 81*, 3036-3046.

DEMETS, C. and S. STEIN, 1990. Present-day Kinematics of the Rivera Plate and Implications for Tectonics in Southwestern Mexico. *J. Geophys. Res., 95*, 21931-21948.

FISHER, R.L., 1961. Middle America trench: Topography and Structure. *Geol. Soc. Am. Bull., 72*, 703-720.

FUENZALIDA, A., M. PARDO, A. CISTERNAS, L. DORBATH, C. DORBATH, D. COMTE and E. KAUSEL, 1992. On the geometry of the Nazca Plate

subducted under Central Chile (32-34.5 S) as inferred from microseismic data. *Tectonophysics, 205*, 1-11.

GETTRUST, J. F., V. HSU, C. E. HESLEY, E. HERRERO and T. JORDAN, 1981. Patterns of seismicity preceding the Petatlán earthquake of 14 March, 1979. *Bull. Seism. Soc. Am., 71*, 761-770.

GOMBERG, J. S., K. M. SHEDLOCK and S. W. ROECKER, 1990. The Effect of S-Wave Arrival Times on the Accuracy of Hypocenter Estimation. *Bull. Seis. Soc. Am., 80*, 1605-1628.

GROW, J. A. and C. O. BOWIN, 1975. Evidence for high density crust and mantle beneath the Chile Trench due to the descending lithosphere. *J. Geophys. Res. 80*, 1449-1458.

HSU, V., C. E. HESLEY, E. BERG and D. A. NOVELO-CASANOVA, 1984. Correlation of foreshocks and aftershocks and asperities. *Pure Appl. Geophys., 122*, 878-893.

KLEIN, R. W., 1978. Hypocenter location program HYPOINVERSE Part I, Users guide to versions 1, 2, 3 and 4. U. S. Geol. Surv. Open File Rep. 78-694.

LEE, W. H. K., R. E. BENNETT and K. L MEAGHER, 1972. A method of estimating magnitude of local earthquakes from signal duration. USGS Open File Rep.

LEE, W. H. K. and C. M. VALDES, 1985. HYPO71PC, A personal computer version of the HYPO71 earthquake location program. USGS Open File Rep., 85-749.

LEFEVRE, L. V. and K. C. MCNALLY, 1985. Stress distribution and subduction of seismic ridges in the Middle America subduction zone. *J. Geophys. Res., 90*, 4495-4510.

LEWIS, B. T. R. and W. E. SNYDSMAN, 1979. Fine Structure of the Lower Oceanic Crust on the Cocos Plate. *Tectonophysics, 55*, 87-105.

LIENERT, B. R., E. BERG and L. N. FRAZER, 1986. HYPOCENTER, An earthquake location method using centered, scaled, and adaptively damped least squares. *Bull. Seism. Soc. Am., 76*, 771-783.

LINDO, R., C. DORBATH, A. CISTERNAS, L. DORBATH, L. OCOLA and M. MORALES, 1992. Subduction geometry in central Peru from microseimicity survey: first results. *Tectonophysics, 205*, 23-29.

LOPEZ-RAMOS, E., 1976. Carta Geológica de la República Mexicana. Instituto de Geología, Universidad Nacional Autónoma de México.

LOPEZ-RAMOS, E., 1983. Geología de México. Tomo III. Mexico City.

LUETGERT, J. H., 1988. User's manual for RAY84/RAY 83PLT, Interactive Two-Dimensional Ray tracing/ Synthetic Seismogram Package, U. S. Geol. Surv. Open File Rep., 88-238, 52 pp.

MAMMERICKX, J. and S. M. SMITH, 1979, Preliminary bathymetry of the East Pacific Rise between 10°N and 18°N. Scripps Institution of Oceanography.

McMECHAN, G.A. and W.D. MOONEY, 1980. Asymptotic ray theory and synthetic seismograms for laterally varying structures: theory and application to Imperial Valley, California. *Bull. Seism. Soc. Am. 70*, 2021-2035.

McNALLY, K. C., J. R. GONZALEZ-RUIZ and C. STOLTE, 1986. Seismogenesis of the 1985 great (Ms=8.1) Michoacán, Mexico earthquake. *Geophys. Res. Lett., 13*, 585-588.

NELSON, G. D., J. E. VIDALE and K. C. McNALLY, 1989. Earthquake Locations by 3-D Finite Difference Travel Time. *EOS, Trans. Am. Geophys. Union, 70* (43).

ORTEGA-GUTIERREZ, F., 1981. Metamorphic belts of southern Mexico and their tectonic significance, *Geofís. Int., 20*, 65-82.

REYES, A., J. N. BRUNE and C. LOMNITZ, 1979. Source mechanism and aftershock study of the Colima, Mexico earthquake of January 30, 1973. *Bull. Seis. Soc. Am., 69*, 1819-1840.

SANDOVAL-OCHOA, J. H., 1985. The Tecpan Regional Fault: Evidence for Major NE Lineaments, *Geofís. Int.*, Special Volume on Mexican Volcanic Belt -Part 1 (Ed. S. P. Verma), *24-1*, 193-202.

SIMILA, G. W., D. A. GARCIA-GONZALEZ, X. LIU, K. C. McNALLY, A. NAVA and E. NAVA. Three-dimensional Velocity Profiling Along the Middle America Trench Offshore Mexico. *EOS, Trans. Am. Geophys. Union, 70* (43), 1989.

SHOR, G. G. and R. L. FISHER, 1961. Middle America trench, Seismic refraction studies. *Geol. Soc. Am. Bull., 72*, 721-730.

SOLTE, C., K. C. McNALLY, J. GONZALEZ-RUIZ, G. W. SIMILA, A. REYES, C. REBOLLAR, L. MUNGUI and L. MENDOZA, 1986. Fine structure of a Post failure Wadati-Benioff Zone. *Geophys. Res. Lett. 13*, 577-580.

SPUDICH, P. and J. ORCUTT, 1980. A new look at the seismic velocity structure of the oceanic crust. *Rev. Geophys. Space Phys. 18*, 627-645.

VALDES-GONZALEZ, C., 1993. Seismic Structure, Scaling, Seismic Attenuation, and Gaps, Using Aftershocks from the major 1979 Petatlán (Ms=7.6) Earthquake. Ph. D. University of Wisconsin-Madison.

VALDES, C. M., R. P. MEYER, R. ZUÑIGA, J. HAVSKOV and S. K. SINGH, 1982. Analysis of the Petatlán aftershocks, energy release and asperities. *J. Geophys. Res., 87*, 8519-8527.

VALDES, C. M., W. D. MOONEY, S. K. SINGH, R. P. MEYER, C. LOMNITZ, J. H. LUETGERT, C. E. HELSLEY, B. T. LEWIS and M. MENA, 1986. Crustal structure of Oaxaca, Mexico, from seismic refraction measurements. *Bull. Seis. Soc. Am., 76*, 547-563.

WEPFER, W., W. and N. I. CHRISTENSEN, 1989. Q Anisotropy in Metamorphic Rocks. *EOS, Trans. Am. Geophys. Union, 70* (15), 1989.

Carlos Valdés-González[1] and Robert P.Meyer[2]
[1] *Instituto de Geofísica, UNAM. Cd. de México, México.*
[2] *Department of Geology and Geophysics, Univeristy of Wisconsin, Madison, USA.*